Impacts of Kermit Conveyor Belt on Mule Deer Habitat Selection, Space Use, and Movement

Daniel R. Eacker[1], and
James W. Cain III [2]

[1] Taurus Wildlife Consulting, Rio Rancho, NM
[2] U.S. Geological Survey, New Mexico Cooperative Fish and Wildlife Research Unit, New Mexico State University, Las Cruces, NM

Cooperator Science Series # 178-2026

About the Cooperator Science Series:

The Cooperator Science Series was initiated in 2013. Its purpose is to facilitate the archiving and retrieval of research project reports resulting primarily from investigations supported by the U.S. Fish and Wildlife Service (FWS), particularly the Office of Conservation Investment. The online format was selected to provide immediate access to science reports for FWS, state and tribal management agencies, the conservation community, and the public at large.

All reports in this series have been subjected to a peer review process consistent with the agencies and entities conducting the research. For U.S. Geological Survey authors, the peer review process (http://www.usgs.gov/usgs-manual/500/502-3.html) also includes review by a bureau approving official prior to dissemination. Authors and/or agencies/institutions providing these reports are solely responsible for their content. The FWS does not provide editorial or technical review of these reports. Comments and other correspondence on reports in this series should be directed to the report authors or agencies/institutions. In most cases, reports published in this series are preliminary to publication, in the current or revised format, in peer reviewed scientific literature. Results and interpretation of data contained within reports may be revised following further peer review or availability of additional data and/or analyses prior to publication in the scientific literature.

The Cooperator Science Series is supported and maintained by the FWS, National Conservation Training Center at Shepherdstown, WV. The series is sequentially numbered with the publication year appended for reference and started with Report No. 101-2013. Various other numbering systems have been used by the FWS for similar but now discontinued report series. Starting with No. 101 for the current series is intended to avoid any confusion with earlier report numbers.

Contractual References:

This document (USGS IPDS #: IP-186901) was developed in conjunction with Atlas Sand Company, LLC and the New Mexico Cooperative Fish and Wildlife Research Unit (U.S. Geological Survey, New Mexico Department of Wildlife, New Mexico State University, U.S. Fish and Wildlife Service and Wildlife Management Institute cooperating). Funding was provided by a grant to J. Cain from the Atlas Sand Company, LLC. New Mexico Department of Wildlife and Bureau of Land Management provided logistical assistance; New Mexico Department of Wildlife also provided capture and field assistance.

Recommended citation:

Eaker, Daniel R. and J.W. Cain III. 2026. Impacts of Kermit Conveyor Belt on Mule Deer Habitat Selection, Space Use, and Movement. U.S. Department of Interior, Fish and Wildlife Service, Cooperator Science Series FWS/CSS-178-2026, Washington, D.C. https://doi.org/10.3996/css72316479

For additional copies or information, contact:

James W. Cain
Department of Rangeland, Wildlife and Fisheries Management, Texas A&M University, College Station, Texas
mail: james.cain@ag.tamu.edu

Impacts of Kermit Conveyor Belt on Mule Deer Habitat Selection, Space Use, and Movement

Photo credit: AP Photo/Julio Cortez

Daniel R. Eacker, Lead Consultant
Taurus Wildlife Consulting, Rio Rancho, NM

James W. Cain III
U.S. Geological Survey New Mexico Cooperative Fish and Wildlife Research Unit
New Mexico State University, Las Cruces, NM (Current affiliation: Department of Rangeland, Wildlife and Fisheries Management, Texas A&M University, College Station, Texas)

July 24, 2026

Contents

List of Tables

List of Figures

List of Appendices

Executive Summary

Technological advancements in hydraulic fracturing and horizontal drilling have created a massive boom in crude oil and natural gas production in the United States. While these developments have succeeded in increasing domestic energy production, they have the potential to negatively impact wildlife populations and the habitats they depend on. Thus, understanding the proximate effects of energy development is imperative to conserving wildlife populations and creating effective mitigation strategies. In 2019, oil and gas production began to grow rapidly in southeast New Mexico due to the extraction of unconventional reserves in the Permian Basin, and this increased truck traffic on local highways. As a mitigation strategy for the high volumes of traffic this created in the region, a conveyor belt system was built spanning 67.6 km that moves sand from a sand mine in Texas to a receiving terminal in New Mexico to support fracking operations. We initiated a pre-post study of mule deer (*Odocoileus hemionus*) using a set of complementary metrics and fine-scale global positioning system (GPS) data to understand the impacts of the Kermit conveyor belt system and right-of-way construction to deer habitat selection, space use, and movement. Like previous studies of mule deer in areas with dense energy infrastructure, we detected a strong signal that deer avoided roads and oil and gas wells in the daytime. After controlling for base habitat selection covariates, we found that mule deer showed strong avoidance for the conveyor belt in the post-construction phase at the population level compared to pre- and active construction phases and a weaker avoidance response to the right-of-way development. We found that even individuals that selected to be closer to the conveyor belt relative to their home range over the study period showed fine-scale avoidance by increasing their minimum distance from the conveyor belt by an average of 555–915 m. We documented this fine-scale avoidance through our space use and distance analysis, which showed that 10% of mule deer locations were within 0.97 km and 1.43 km of the conveyor belt on average in the pre- and post-construction phases, respectively. Concurrently, we found that the proportion of high use area declined in the active and post-construction phases compared to the pre-construction phase for both features by factors of 4.8%–27.3%. We used barrier behavior analysis to examine how deer behaviorally responded to the conveyor belt and right-of-way construction as barriers to movement. Although we did not observe any changes in the frequency of normal or altered behaviors, we detected a significant effect on the number of 50-m sections of conveyor belt route that were encountered between the pre- and post-construction phases. For instance, less than a third of the wildlife crossing structures built in areas that were used by collared animals in the pre-construction phase were used post-construction, and the western portion of the belt had no encounter events after the conveyor belt was complete. We attribute this decline in encounter events to the fine-scale avoidance that deer showed toward the conveyor belt. In summary, it appears that the Kermit conveyor belt had significant negative effects on mule deer by causing deer to avoid the conveyor belt and reducing their ability to move across the landscape, further constraining deer populations in an area that has already seen substantial habitat alterations. Without future mitigation efforts, deer populations may experience

declines like other areas in Intermountain West where habitat degradation has occurred from energy development. Improvements to wildlife crossing structures may help mitigate the impact of the conveyor belt, and continued monitoring of wildlife crossings and mule deer populations in response to mitigation strategies will be necessary to evaluate their efficacy.

Keywords: avoidance, conveyor belt, energy development, habitat selection, mule deer, New Mexico, *Odocoileus hemionus*, resource selection function, right-of-way, ungulate.

Introduction

As human development proliferates, understanding the potential negative impacts to wildlife populations becomes imperative to conservation and mitigation efforts. Often, development creates barriers for wildlife species that impair their ability to move across the landscape (Harrity et al. 2024), potentially leading to altered behavior (Robb et al. 2022), habitat loss and fragmentation (Lovich and Ennen 2011), and population declines if reduced landscape permeability results in restricted access to essential resources (Hebblewhite 2017). Since the early 2000s, energy development due to advances in hydraulic fracturing (i.e., fracking) technology, combined with horizontal drilling, has created a massive boom in crude oil and natural gas production in the United States (Cook et al. 2018) that has the potential to dramatically alter landscapes for wildlife (Allred et al. 2015). Ungulate species may especially be at risk because of their sensitivity to landscape disturbances resulting from their relatively large space-use requirements. However, because declines in abundance of ungulate populations generally happen over longer timescales than most monitoring studies and can be influenced by climatic variation (Hurley et al. 2017, Schuyler et al. 2019), causal relationships between wildlife space use and demography and the growth in energy development may be more difficult to detect, especially if avoidance of these energy features occurs (e.g., Skelly et al. 2024). Thus, indirect effects such as changes in habitat availability, habitat selection, movement rates or other avoidance behaviors provide metrics to quantify the proximate effects of infrastructure development on ungulates.

Mule deer (*Odocoileus hemionus*) are a prominent focus of impacts from oil and gas developments in the Intermountain West because of direct reductions in critical winter range habitat (Northrup et al. 2015), overall population declines (Sawyer et al. 2017), and their sensitivity to human disturbance relative to other ungulates (Sawyer et al. 2019). Numerous studies in western Wyoming have found that mule deer avoid or are displaced by oil and gas development and their associated infrastructure such as roads (Sawyer et al. 2006, 2009, 2017; Northrup et al. 2015, 2021; Dwinnell et al. 2019). Because of these avoidance behaviors, the realized loss of winter range and critical forage resources is greater than the actual loss due to the combined footprint of oil and gas infrastructure. Studies suggested that these avoidance effects may be attenuated in more rugged terrain that provide pockets of refugia for deer (Northrup et al. 2015), and as such may explain the disparity in the avoidance distances found between recent studies in more complex terrain (i.e., 800 m; Northrup et al. 2015) compared to flatter, more open terrain (2–3 km; Sawyer et al. 2006). Northrup et al. (2015) also decomposed active drilling vs. production phases and oil and gas well sites and day and night periods for deer habitat selection, finding that deer avoidance for oil and gas sites declined after active drilling concluded and that they avoided roads more in the day compared to night. Combined, these disturbances to mule deer winter range result in reduced carrying capacity that appears to be a significant driver of a decades-long decline in populations in the region, where abundance has declined by 36% during the development period (Sawyer et al. 2017). Although these effects of oil and gas development are well-known in sagebrush steppe habitats, less is known about how mule deer populations might respond to similar developments in southwestern deserts and arid environments where forage resources are more limited.

Oil and gas production has increased in New Mexico in the Permian Basin, mirroring the rapid development of unconventional shale resources in Wyoming and in the Bakken Formation in Montana and North Dakota. During 2019–2024, New Mexico became the second largest producer of oil in the United States, with the industry's growth greatly exceeding Texas. Oil production rose from 0.9 million barrels per day (mb/d) in 2019 to 2.0 mb/d in 2024. Exploration has largely occurred in Eddy and Lea counties on federal lands in the southeast corner of the state, which accounts for two-thirds of crude oil production (Godling et al. 2025). As a result of this growth, truck traffic increased greatly in the region due to the need to haul sand and water to fracking sites. As a mitigation measure to reduce traffic, emissions and safety hazards on local roads, a sand conveyor belt was built spanning 67.6 km known as the *Dune Express* that moves sand from the Atlas Kermit sand mine in Winkler County, Texas, to a receiving terminal in Lea County, New Mexico to support fracking operations. In an area where mule deer already contend with a matrix of roads and oil and gas well sites, and arid environmental conditions, the potential for this extensive linear feature to create barriers and disrupt mule deer movement could be significant. Because the Kermit conveyor belt represents a unique structure in the United States, there are no case studies to predict how deer might respond. However, studies of wildlife responses to above ground pipelines from Alberta's oil sands included analyses of over-pipeline crossing structures (Dunne and Quinn 2009) and a focus on how variation in the height of the pipeline affected mammalian movement rates (Charleboi et al. 2023). They found that deer (*Odocoileus* spp.) crossing rates were 83.1%–94.9% with average pipe clearance of 1.2–1.5 m, but it was unclear whether these results were more driven by mule or white-tailed deer (*Odocoileus virginianus*) in Dunne and Quinn (2009) because the authors group data from both species together. Deer could become habituated to certain energy infrastructure, but it is uncertain if deer would respond similarly to a sand conveyor belt that may generate more noise and create a more substantial barrier given the lack of clearance under much of the length of the structure.

To address the potential impact of the Kermit conveyor belt we carried out a pre-post study in southeast New Mexico using a comprehensive approach to evaluate how the conveyor belt and right-of-way (ROW) construction influenced deer habitat selection, space use, and movement. Our habitat selection analyses tested for changes in selection for distance to the conveyor belt and ROW in the pre-, active, and post-construction phases. We predicted that deer would select for areas farther from the conveyor belt post-construction compared to pre- and active-construction phases. We predicted the effect would be stronger for the conveyor belt compared to the ROW because deer could easily cross the ROW whereas the conveyor belt presented a potentially significant barrier for deer. Like other studies that examined the effects of oil and gas infrastructure on mule deer habitat selection (Sawyer et al. 2006, 2009; Northrup et al. 2015), we predicted that deer would select for greater distance during the day compared to night for both roads and oil and gas well sites given greater human activities during the day. We also explored change in high use area and the proportion of locations within increasing distance buffers of the conveyor belt (*sensu* Sawyer et al. 2025). To evaluate fine-scale impacts of the conveyor belt as a potential barrier to movement, we utilized Barrier Behavior Analysis (BaBA), a new approach to detect the effects of linear barriers on animal movements (Xu et al. 2021).

Study Area

Our study area (~9,791 km^2) occurred along the New Mexico-Texas border in southeastern New Mexico and west-central Texas on the northern periphery of the Chihuahuan Desert (32.028 N, 103.518 W; Fig. 1) and had an arid climate that experienced large diurnal and seasonal oscillations in temperature and precipitation. Elevation across the study site ranged from 859–1,119 m. Annual temperatures ranged from 9.1℃ to 24.8℃ with 33.0 cm of accumulated precipitation based on climate normals from 2006–2020. The conditions during our study were average for temperature with minimums of 8.8℃ to 10.1℃ and maximums of 24.4℃ to 28.1℃ and below-average precipitation ranging from 2.9 cm in 2024 to 5.7 cm in 2025, representing moderate to severe drought conditions (ncei.noaa.gov, accessed 2 April 2026). Most precipitation occurs in the late spring and monsoon seasons during June to September when heavy rainfall can occur sporadically over the landscape resulting in unpredictable temporal and spatial variation in forage resources.

The region was categorized as the Chihuahuan Basins and Playas Ecoregion and included alluvial fans, internally drained basins, and low-elevation river valleys (Griffith et al. 2004, 2006). The landscape was composed of salt flats, dunes, and windblown sand and was dominated by creosote bush (*Larrea tridentata*). Common shrubs and grasses include tarbush (*Flourensia cernua*), fourwing saltbush (*Atriplex canescens*), acacias (*Acacia* spp.), gypsum grama (*Bouteloua breviseta*), and alkali sacaton (*Sporobolus airoides*), with horse crippler (*Echinocactus texensis*) and other cacti also considered common (Griffith et al. 2006). The study area also intersected a small portion of sand shinnery habitat that was dominated by shin-oak (*Quercus havardii*), of which the acorns, buds, and leaves are known to be a principal food source for mule deer (Peterson and Boyd 1998).

The study area lies within the Permian Basin, an expansive sedimentary basin that has an extensive human footprint and is the leading oil and gas resource in the United States. Along with the development of the 67.6-km-long Kermit conveyor belt system, the area contained a high-density of gas and oil wells (1–82/km^2) and roads (0.11–5.54 km/km^2; Villarreal et al. 2023; rrc.texas.gov, accessed 12 June 2025).

Methods

The conveyor belt was designed to move sand back and forth at 16 kilometers per hour from a loading station near Kermit, Texas, to a receiving facility on the western end of the belt in New

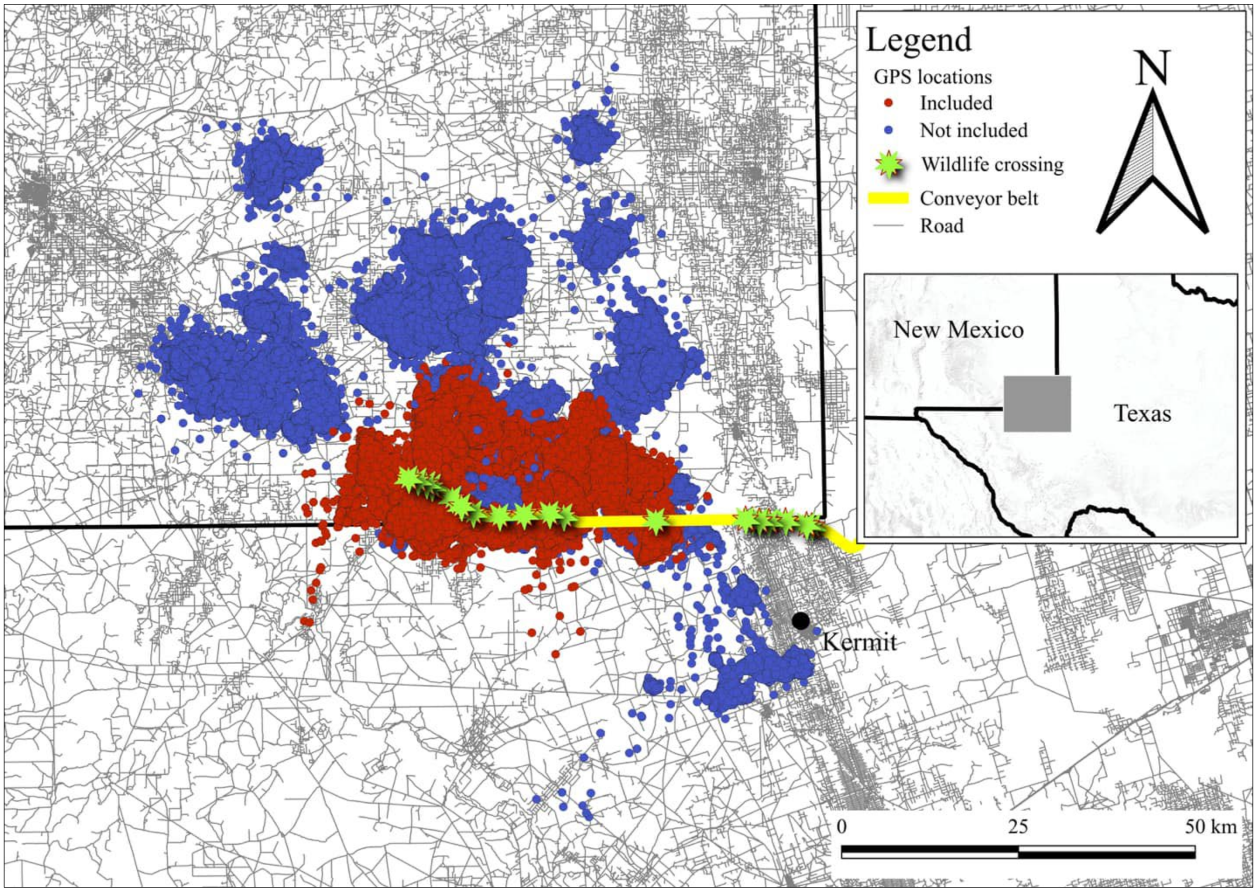

Figure 1. Study area in southeastern New Mexico and west-central Texas including locations from GPS-collared adult mule deer (March 2022 ─ 21 February 2025), wildlife crossing structures, and roads and the Kermit conveyor belt system. Note that GPS locations are stratified by those that were included in the analysis (red points) and those not included (blue points).

Mexico (see Fig. 1). A ROW that was approx. 22-m wide was cleared before conveyor belt construction began and was completed incrementally as different sections of the conveyor belt were built. The base supports for the conveyor belt were 3.3-m wide, and the conveyor belt was 1.4-m wide. The standard ground modules of the conveyor belt had a height of 1.8 m and were spaced 4.9-m apart, with 0.7 m of clearance below the lower return belt. The height increased in sections to accommodate traffic and wildlife crossing structures, with 7.6 m of clearance across a span of 39.0 m and 3.5 m of clearance across a span of 14.6 m, respectively.

We used high-resolution imagery captured from drone flights of the construction area conducted 1–3 times per month (n = 28) during 18 June 2023 to 5 August 2024 to separately digitize the conveyor belt and ROW during active construction. We used QGIS (QGIS

Development Team 2025) to create linestring and polygon features for the conveyor belt and ROW, respectively. These date-specific spatial features allowed us to extract time-varying distance covariates across construction phases for both the conveyor belt and ROW. We delineated the pre- and post-construction phases for the conveyor belt and ROW based on the digitized drone imagery rather than exact dates of initiation and completion of the development. Thus, conveyor belt construction began 15 August 2023, was finished 1 October 2024, and ROW construction began 21 March 2023 and was finished 6 June 2024.

Adult Capture and Monitoring

We captured 97 (77 female, 20 male) adult mule deer using helicopter netgunning in March 2022; we captured an additional 21 adult female mule deer in March 2023 to replace study animals lost to mortality. We fitted all deer with GPS-Iridium collars (Litetrack Iridium 420, Lotek Wireless Inc., Newmarket, Ontario, Canada) and released them at the point of capture. All mule deer capture and handling methods were approved by the New Mexico State University Institutional Animal Care and Use Committee (Protocol 2022-002).

Although additional deer were caught farther away (i.e., maximum distance from conveyor belt = 63.7 km), we focused the analysis on individuals in proximity to the conveyor belt (i.e., maximum distance from conveyor belt = 24.7 km; see Fig. 1) that did not exhibit increased movement due to rut or seasonal migratory behaviors and that had data coverage over the construction phases. Thus, we excluded individuals that had <100 locations within a construction period, and we visually inspected movement tracks to determine proximity to the conveyor belt and net-squared displacement plots to screen for movement anomalies.

GPS collars were initially programmed to collect fixes every 3 hours, with every other GPS position transmitted via Iridium satellite every 2–3 days. However, to reduce costs associated with uploading locations to the Iridium network, some collars were changed to a 6-hr fix rate. However, this did not affect our habitat selection analysis because all relocation data were rarefied to a common 6-hour fix rate for this analysis. We removed any GPS locations that occurred 48 hours directly after capture and any locations after the collar had dropped off or a mortality had occurred. We filtered out low accuracy locations before analysis by only including 3-dimensional fixes with dilution of precision ≤4 (Jung et al. 2018), which a represented 6.0% reduction in our dataset.

Home Ranges

We used dynamic Brownian bridge movement models (dBBMMs) to fit utilization distributions (UDs) to mule deer location data using the 'move' package (Kranstauber 2024) in program R (R Core Team 2025). Because we had variable fix rates across individuals, we adjusted the window size by dividing a 47-hour period by the median GPS fix rate, rounding the result, and adding one if the result was even (e.g., 3-hour fix rate: $[47/3] + 1 = 17$ locations). Similarly, for the margin we divided the window size by 3.5, rounded the result, and added one if the result was even (e.g., $[17/3.5] = 5$ locations). These window size and margin settings represented a biologically relevant time frame to detect diurnal changes in motion variance and larger movements that may have occurred in response to development (Kranstauber et al. 2012).

Habitat Selection

We used a 3rd-order habitat selection analysis in a used-available design to control for variables known to be important to mule deer and test for avoidance of conveyor belt and ROW features (Johnson 1980, Manly et al. 2002). Using similar methods as our space-use analysis, we fit home ranges to each individual's entire location set to define availability. We reasoned that if an individual shifted their activity area away from the conveyor belt or ROW over the construction phases (i.e., avoidance), that the distance they selected for would increase in the post-construction phase relative to pre-construction in comparison to the distances available over the entire period (Fig. 2). We chose not to block availability by seasonal periods because we filtered out individuals that exhibited seasonal movements and this would have limited our ability to detect avoidance of the development features by constraining availability to a relatively small area. We used a 1:5 used-to-available point ratio in our analysis (Shanley et al. 2021), which was provided ample coverage to represent availability over the home ranges in our study. We used the 'amt' (Singer et al. 2019) and 'sf' (Pebesma 2018, Pebesma and Bivand 2023) packages in R to rarify data to a common 6-hr fix rate and sample random points from individual home ranges, respectively.

We used generalized linear mixed-effects models (GLMMs) and included random intercepts and slopes for individual deer to estimate population-level resource selection function (RSF) coefficients (Gilles et al. 2006). By including random individual slopes, we were able to account for the fact that not all individuals might respond similarly to the conveyor belt and ROW developments, while also being able to describe the average response of the population. This approach also allowed us to account for the slightly unbalanced sample across individual deer and the pseudoreplication from repeated sampling of individuals (Muff et al. 2019). Following Manly et al. (2002), we used an exponential function of continuous covariates (x_n) and regression coefficients ($\hat{\beta}_n$) to predict a vector of weights ($\hat{w}$) that represented relative selection for resources at a set of locations (s):

$$\hat{w}(s) = \exp(\hat{\beta}_0 + \hat{\beta}_1 x_1 + \hat{\beta}_2 x_2 + \hat{\beta}_n x_n) \tag{1}$$

We specifically used a logit link function to model our binary response variable (i.e., 1 = used, 0 = available) as a linear function of a set of continuous predictor covariates following:

$$\mathrm{logit}(y_{ij}) = (\beta_0 + \gamma_{0j}) + x_{nj}(\beta_n + \gamma_{nj}) \tag{2}$$

where the i^{th} observation is clustered within the j^{th} individual deer in a two-level random-effects structure (Gillies et al. 2006). In this formulation, β_0 is the grand mean intercept; β_n is the fixed,

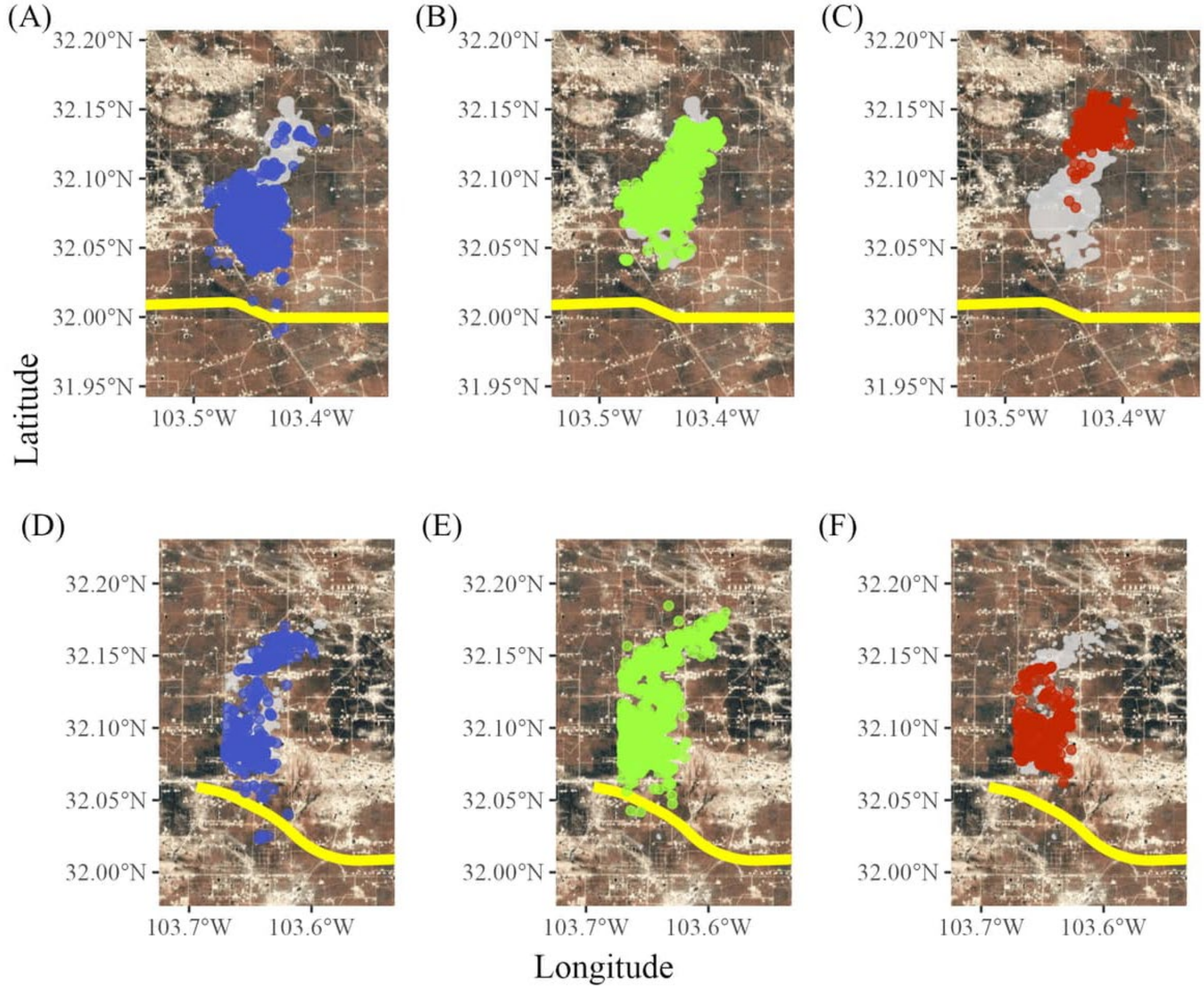

population-level coefficient for the n^{th} predictor covariate (x_{nj}) for individual j; and γ_{0j} and γ_{nj} are the random intercept and slopes, respectively, for the j^{th} individual and n^{th} coefficient. The

Figure 2. Mule deer GPS locations for two individuals with contrasting responses to conveyor belt development given availability defined by their home range over the entire study period (transparent white polygons). The upper panels for the first individual show selection changing from (A) negative ($\beta = -3.9$), to (B) neutral ($\beta = 0.1$), and then to (C) positive ($\beta = 2.8$) for distance to conveyor belt in the pre- (blue points), active (green points), and post-construction (red points) phases, with positive selection indicating avoidance for the feature. The lower panels for the second individual show selection changing from (D) positive ($\beta = 1.2$), to (E) neutral ($\beta = 0.0$), and then to (F) negative ($\beta = -2.1$), with negative selection indicating preference for closer distance to the feature. Note that the conveyor belt is shown as a yellow line.

random intercepts and slopes are assumed Gaussian distributed (Hosmer and Lemeshow 2000), and we specified no correlation between the random slopes and intercepts as the intercept had no biological interpretation in our model (Gillies et al. 2006).

We used the R package 'glmmTMB' (Brooks et al. 2017) to estimate parameters for GLMMs which implements maximum likelihood estimation. We scaled continuous predictors by one standard deviation and centered them at zero to compare relative effect sizes. As recommended in Muff et al. (2019), we assigned a set of model weights of 1 for used and 1,000 for available locations. Finally, we used Google Compute Engine on the Google Cloud (Google 2025) to allow for high memory and multicore processing of our relatively large dataset and complex models.

Model Selection and Covariates

We restricted habitat selection analyses for both conveyor belt and ROW construction to only include individuals that occurred in all three phases of construction. This allowed us to test for an interaction between distance to the development features and the construction phase while accounting for individual responses in a unified model. We used the Bayesian Information Criteria (BIC; Schwart 1978) and a *k*-fold cross-validation routine (Boyce et al. 2002) as support criteria for the top model. For our cross-validations, we blocked by individual deer and fit models to 80% of individuals as training data and withheld 20% of individuals as the test data for each fold. We used 5-fold cross-validation and calculated the mean Spearman's rank correlation coefficient ($\bar{\rho}$) across the trials. We first considered base covariates with or without day or night and seasonal interactions (Table S1 in Appendix). We developed the base model sequentially by selecting the top formulation based on $\bar{\rho}$ and BIC for each covariate out of four candidate models that included: the main effect; an interaction with the main effect and day/night; an interaction with the main effect and season; and an interaction with the main effect, day/night, and season. Building on the base model, we then used a similar model selection strategy for human disturbance variables that were prominent features that deer might show avoidance to in the study area. After selecting the most predictive form of base and human disturbance models, we tested for the interactive effects of distance to conveyor belt and ROW and the respective construction phases and considered models with an interaction of day/night and the construction phase. Finally, although it was not our primary focus of the analysis, we fit models that included distance to wildlife crossings as the treatment covariate in the place of distance to conveyor belt and ROW. Distance to wildlife crossings had to be included separately because it was inherently correlated with distance to conveyor belt and ROW in the pre- and post-construction phases. We tested for collinearity between our continuous covariates using a Pearson's correlation coefficient ($\hat{r}$) and considered $|\hat{r}|$ <0.7 as a cutoff for variable inclusion (Dormann et al. 2013).

Base covariates and temporal strata

We controlled for a suite of covariates known to be important to mule deer habitat selection, which we considered base covariates and included in all models in the analysis. We considered elevation, Soil Adjusted Vegetation Index (SAVI), distance to water, and percent cover of shrubs between 0.5–2.0 m in height. We downloaded a Digital Elevation Model (DEM) from NASA that had 30-m resolution over the study area (NASA JPL 2021). We downloaded SAVI from Landsat

8-9 satellite data using the R package ‘rLandsat’ (Skaria et al. 2026). SAVI is preferred in areas where vegetative cover is low such as in our study area and is used to correct the Normalized Difference Vegetation Index for the influence of soil brightness (USGS 2025). We mosaiced and cropped SAVI tiles using the ‘terra’ package in R and then extracted the time-specific values for our used-available dataset. Water vector data were downloaded from the New Mexico Environment Department (https://www.env.nm.gov, accessed 12 June 2025) and from the Texas Railroad Commission (https://www.rrc.texas.gov, assessed 8 June 2025), and then combined and clipped for the study area. We then calculated distance to water using the *shortest line between features* function in QGIS. For percent shrub cover between 0.5–2.0 m, we acquired 2023 LANDFIRE data for vegetation height and percent cover (https://www.landfire.gov, assessed 10 June 2025). We then extracted the values for percent shrub cover and filtered by heights.

We used the R package ‘suntools’ (Bivand and Luque 2025) to create the day/night indicator variable by calculating civil dawn and dusk times based on the timestamps of our GPS dataset. This approach yielded 54.8% and 45.2% classified as day and night locations, respectively. We defined four seasonal periods as monsoon (July–September), rut (October–January), winter (February–March), and spring (April–June) based on expert opinion (J. W. Cain, personal communication, 12 March 2026).

Human disturbance covariates

We considered roads and oil and gas well locations as the primary human disturbances in the study area given their relatively large footprint. Oil and gas locations along with primary and secondary roads were provided by U.S. Geological Survey (USGS) geodatabase from the Carlsbad Field Office in New Mexico (Villarreal et al. 2023). Similar data were available from the Railroad Commission of Texas (rrc.texas.gov, accessed 12 June 2025) where we downloaded data for the 5 counties nearest to our study area and clipped them for our study area extent. These layers were then combined, and distance metrics were extracted using the same approach as for water features.

Treatment covariates

We used the linestring and polygon vector data that were digitized from drone imagery to estimate distance metrics for treatment conveyor belt and ROW features. In the pre- and post-construction phases, we calculated distances based on the completed features, while we used time-specific distances in the active phase to accurately account for the progress of construction through time. We matched up our 6-hr fix locations to the closest drone survey date, which had a ~2-week interval between surveys ($\bar{x}$ = 15.5 days, SD = 5.2 days). We calculated distance to wildlife crossing structures (m) like other distance metrics.

Space-use Patterns

We developed population-level estimates of space use by averaging over normalized individual UDs in the pre-, active, and post-construction phases and calculating the cumulative distribution functions. We then extracted the contour for the upper 30% of cumulative distribution function values as polygon features to visualize changes in high-use areas. Following Sawyer et al. (2025), we used distance bands of 1-, 2-, and 3-km to determine the proportions of the population-level UDs that were within these buffers to compare high-use area relative to total acreage in the pre-, active, and post-construction phases for both the conveyor belt and ROW.

Distance Analysis

We calculated the proportion of locations within 3-km of the conveyor belt and ROW using 10-m increments to create distance buffers to test for the potential avoidance by deer that were in proximity of the development features. For consistency with our RSF analysis, we based this analysis on our 6-hr location dataset for each of the three construction phases. We plotted individual and average proportion of locations within buffer distances (n = 300, range = 10–3,000 m) to visualize these potential fine-scale effects on behavior.

Because our 3rd-order home range analysis may not detect fine-scale avoidance, we also calculated the average difference in the minimum distance across individuals between pre- and post-construction phases for conveyor belt and ROW features. We summarized these average shifts in minimum distances based on the following criteria: 1) negative to positive selection, 2) positive to negative selection, 3) maintaining negative selection, or 4) maintaining positive selection for distance to the feature. We considered an average shift of 600-m or greater between pre- and post-construction phases for individuals that switched from negative (i.e., preference) to positive (i.e., avoidance) selection to be consistent with other studies that documented fine-scale avoidance of energy development features (Northup et al. 2015, Sawyer et al. 2017).

Barrier Behavior Analysis

As an additional fine-scale test, we used a Barrier Behavior Analysis (BaBA) to assess the potential for the conveyor belt and ROW to result in a barrier to movement for deer. This method classifies barrier encounters into six categories: quick cross, average movement, bounce, back-and-forth, trace, and trapped (Fig. 3; Xu et al. 2021). We removed the trapped classification from our analysis given this category was developed for fence barriers. Because GPS data with course fix rates (e.g., 6-hr) can misclassify altered movements as normal (e.g., a trace event that is classified as a cross when the animal finally is able to cross), we focused this analysis only on the subset of individuals with a 3-hr fix rate. As suggested in Xu et al. (2021), we conducted a sensitivity analysis to determine the ideal buffer distance based on the change in the number of quick crosses as the buffer distance was increased. We split the conveyor belt feature into 50-m segments using the ‘stplanr’ (Loveless and Ellison 2018) package in R and used the ‘BaBA’ package (Xu and Hermann 2026) to classify encounter events and calculate an impermeability index for the conveyor belt segments (see Xu et al 2021 for details). We choose not to use the default settings to calculate the impermeability index that weights the index by the number of individual animals along the fence section because of the relatively low number of unique individuals that encountered the conveyor belt. Thus, the impermeability index was calculated as

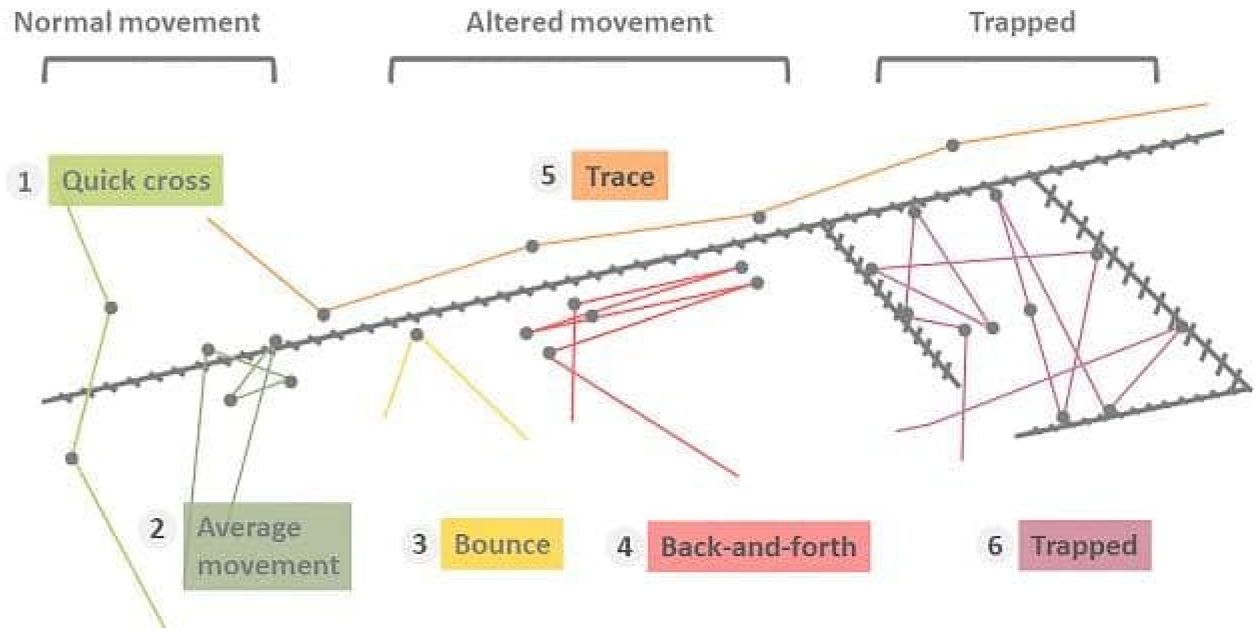

the ratio of altered movements (bounce, back-and-forth, and trace) to total encounters and rescaled between zero and one. Finally, because the duration and number of fixes varied by belt and ROW construction phases, we focused our comparison of encounter events on monthly rates, which had more balanced sample sizes.

Figure 3. Behavior classifications in Barrier Behavior Analysis (BaBA) borrowed from Xu et al. (2021) showing normal (quick cross and average movement), altered (bounce, back-and-forth, and trace), and trapped movements.

Results

Habitat Selection Analysis

After screening movement data and removing two individuals that had few locations in the post-construction phase (n_{loc} <67), we had 33 adult deer of both sexes (30 female, 3 male) in our 3rd-order habitat selection analysis of conveyor belt disturbance effects. Our GPS dataset for the conveyor belt analysis contained 109,448 used locations and 29,658 animal-days spanning 8 March 2022 to 21 February 2025 (Table 1). Adult male and female mule deer in this portion of the analysis had mean home range sizes of 34.6 km^2 (SD = 20.3 km^2) and 32.2 km^2 (SD = 11.2 km^2), respectively, based on the 95% UDs. Because construction was delayed, we had fewer GPS locations in the post-construction phase compared to pre- and active construction phases (Table 1).

In our conveyor belt RSF analysis, we found some support for day/night and seasonal interactions with base covariates based on k-fold cross-validations, which we considered more reliable than the BIC that invariably supports the most complicated models with large GPS datasets (see Table S2 in Appendix). Across all models, SAVI was the strongest base predictor of deer habitat selection, having a Spearman's rank correlation coefficient ($\bar{\rho}$) in a univariate model of 0.92. Intuitively, the coefficient for SAVI was positive with deer selecting for greater values of SAVI that represented greater vegetation productivity, and the selection for SAVI was slightly stronger during the day compared to the night (Table 2). The next most-important base covariate was distance to water with deer having relatively strong selection for closer distance to water in the monsoon season. Although included as base covariates, percent shrub cover between 0.5–2.0 m height and elevation were not important for deer habitat selection based on statistical significance (Table 2). We retained day/night interactions with distance to road and oil and gas wells given model selection support (Table S2). After accounting for base covariates, we found that deer selection for roads depended on day/night, with deer avoiding roads in the day being significant. Deer had a relatively weak response to oil and gas wells that also depended on day/night, with deer having moderately significant selection for closer distance to wells at night.

Table 1. Summary of number of used locations (n_{loc}), and mean and standard deviation of number of locations per individual, and animal-days of GPS data in the pre-, active, and post-construction phases for the conveyor belt (Belt) and right-of-way (ROW) analyses.

Analyses	Phase	n_{loc}	$\bar{x}$ (SD)	Animal-days
Belt	Pre	45,495	1,378.6 (690.7)	12,348
Belt	Active	50,147	1,519.6 (108.9)	13,627
Belt	Post	13,806	418.4 (55.0)	3,680
ROW	Pre	30,442	1,383.7 (91.6)	8.279
ROW	Active	35,746	1,624.8 (131.5)	9,744
ROW	Post	17,680	803.6 (167.2)	4,793

Even with a relatively limited post-construction data (i.e., 4 months), we found strong evidence that deer avoided the conveyor belt in the post-construction phase, with distance to conveyor belt having the largest standardized coefficient of any variable included in the fully saturated model (Table 2). Importantly, the population-level response to the construction changed over time, going from negative (i.e., selection for closer distance) in the pre-construction phase, to neutral during active construction, to strong avoidance in the post-construction phase (Table 2, Fig. 4). Responses to conveyor belt construction varied across individuals in the pre- and post-phases (Fig. 5). We estimated that 30.3% of individuals (10/33) selected to be closer to the conveyor belt in the pre-construction phase and then switched to avoidance post-construction; 39.4% of individuals (13/33) showed avoidance in the pre- and post-construction phases; 18.1% of individuals (6/33) showed selection for closer distance to the conveyor belt in the pre- and post-construction phases; and 12.1% of individuals (4/33) switched from avoidance in the pre-construction phase to selecting for closer distance in the post-construction phase (Fig. 5). We found that selection for distance to wildlife crossings was not important in any conveyor belt construction phase.

For our analysis based on the ROW construction phases, we had 22 adult deer of both sexes (19 female, 3 male) after screening movement data and removing one individual that had few locations in the post-construction phase (n_{loc} = 96). Our GPS dataset for the ROW analysis contained 83,868 used locations and 22,820 animal-days spanning 8 March 2022 to 21 February 2025 (Table 1). Adult male and female mule deer in this portion of the analysis had home range sizes of 34.6 km^2 (SD = 20.3 km^2) and 34.0 km^2 (SD = 11.7 km^2), respectively, based on the 95% UDs.

Like the conveyor belt, we had fewer GPS locations for the ROW construction phases in the post-construction phase compared to pre- and active phases because of delays in construction (Table 1). Our results for the effects of distance to ROW on deer habitat selection generally mirrored those of the conveyor belt feature, but with a more attenuated response by deer in the post-construction phase. Again, we found some support for day/night and seasonal interactions with base covariates based on *k*-fold cross-validations (see Table S3) with SAVI being the strongest predictor and a Spearman's rank correlation coefficient ($\bar{\rho}$) in a univariate model of 0.95. Deer selection for SAVI was near identical for the ROW compared to the conveyor belt analyses with slightly stronger selection during the day compared to the night (Table 3). We found that elevation and % shrub cover between 0.5–2.0 m height had no importance for deer

Table 2. Standardized population-level coefficient estimates ($\hat{\beta}$), 95% lower (LCI) and upper (UCI) confidence intervals, and *P*-values from generalized mixed-effects models including: elevation (m); Soil-Adjusted Vegetation Index (SAVI) in the day and night; percent (%) shrub cover between 0.5–2.0 m in the day and night; distance to water (m) in monsoon, rut, winter, and spring seasons; distance to road (m) in day and night; distance to oil and gas wells (m) in the day and night; and distance to conveyor belt (m) in pre-, active, and post-phases of conveyor belt construction.

Covariate	$\hat{\beta}$	LCI	UCI	*P*
Elevation	0.243	−0.175	0.661	0.255
SAVI:Day	0.497	0.388	0.607	<0.001
SAVI:Night	0.409	0.298	0.520	<0.001
Shrub cover (%):Day	0.022	−0.047	0.092	0.530
Shrub cover (%):Night	0.014	−0.061	0.089	0.707
Distance to water:Monsoon	−0.337	−0.620	0.053	0.020
Distance to water:Rut	−0.197	−0.464	0.070	0.148
Distance to water:Winter	0.021	−0.271	0.312	0.890
Distance to water:Spring	−0.235	−0.501	0.063	0.084
Distance to road:Day	0.400	0.239	0.562	<0.001
Distance to road:Night	0.085	−0.009	0.178	0.075
Distance to oil and gas wells:Day	0.082	−0.012	0.176	0.089
Distance to oil and gas wells:Night	−0.055	−0.104	−0.006	0.029
Distance to conveyor belt:Pre	−0.317	−0.679	0.046	0.087
Distance to conveyor belt:Active	0.009	−0.013	0.031	0.415
Distance to conveyor belt:Post	0.703	0.176	1.229	0.009

habitat selection, while distance to water was significant in the spring with an equally large but non-significant response in the monsoon season as deer selected to be closer to water (Table 3). Again, we retained day/night interactions with distance to road and oil and gas wells given model selection support (Table S3). Human disturbance metrics had stronger effects during the daytime compared to night. Deer showed significant avoidance of roads and oil and gas wells in the day but not at night, with especially strong selection for farther distance from roads (Table 3).

We found no statistical evidence that deer avoided the ROW in active or post-construction, with only weak avoidance in both phases (Table 3). At a population level, deer showed strong selection to be closer to the ROW in the pre-construction phase relative to their home range over the entire study period (Table 3, Fig. 4). Responses to conveyor belt construction varied across individuals but mostly in the pre-construction phase, with nearly half the individual variation in the post-construction phase of the ROW (σ = 0.71) as compared to the conveyor belt (σ = 1.54; Fig. 5). Although the population-averaged effect was attenuated in the ROW habitat selection analysis, we estimated that 31.8% of individuals (7/22) selected to be

Table 3. Standardized population-level coefficient estimates ($\hat{\beta}$), 95% lower (LCI) and upper (UCI) confidence limits, and *P*-values from generalized mixed-effects models including: elevation (m) in day and night; Soil-Adjusted Vegetation Index (SAVI) in day and night; percent (%) shrub cover between 0.5–2.0 m in monsoon, rut, winter, and spring seasons; distance to water (m) in monsoon, rut, winter, and spring seasons; distance to road (m) in the day and night; distance to oil and gas wells (m) in the day and night; and distance to right-of-way (m) in the pre-, active, and post-phases of right-of-way construction.

Covariate	$\hat{\beta}$	LCI	UCI	*P*
Elevation:Day	0.407	−0.145	0.959	0.148
Elevation:Night	0.439	−0.078	0.956	0.100
SAVI:Day	0.485	0.346	0.625	<0.001
SAVI:Night	0.425	0.293	0.557	<0.001
Shrub cover (%):Monsoon	−0.053	−0.132	0.025	0.180
Shrub cover (%):Rut	0.031	−0.043	0.105	0.409
Shrub cover (%):Winter	−0.015	−0.114	0.084	0.761
Shrub cover (%):Spring	−0.002	−0.075	0.071	0.959
Distance to water:Monsoon	−0.315	−0.655	0.026	0.070
Distance to water:Rut	−0.072	−0.328	0.184	0.582
Distance to water:Winter	0.067	−0.186	0.321	0.603
Distance to water:Spring	−0.303	−0.558	−0.048	0.020
Distance to road:Day	0.258	0.119	0.398	<0.001
Distance to road:Night	−0.006	−0.085	0.072	0.874
Distance to oil and gas wells:Day	0.138	0.029	0.247	0.013
Distance to oil and gas wells:Night	−0.035	−0.090	0.020	0.208
Distance to right-of-way:Pre	−0.547	−1.034	−0.059	0.028
Distance to right-of-way:Active	0.116	−0.081	0.314	0.248
Distance to right-of-way:Post	0.110	−0.190	0.403	0.481

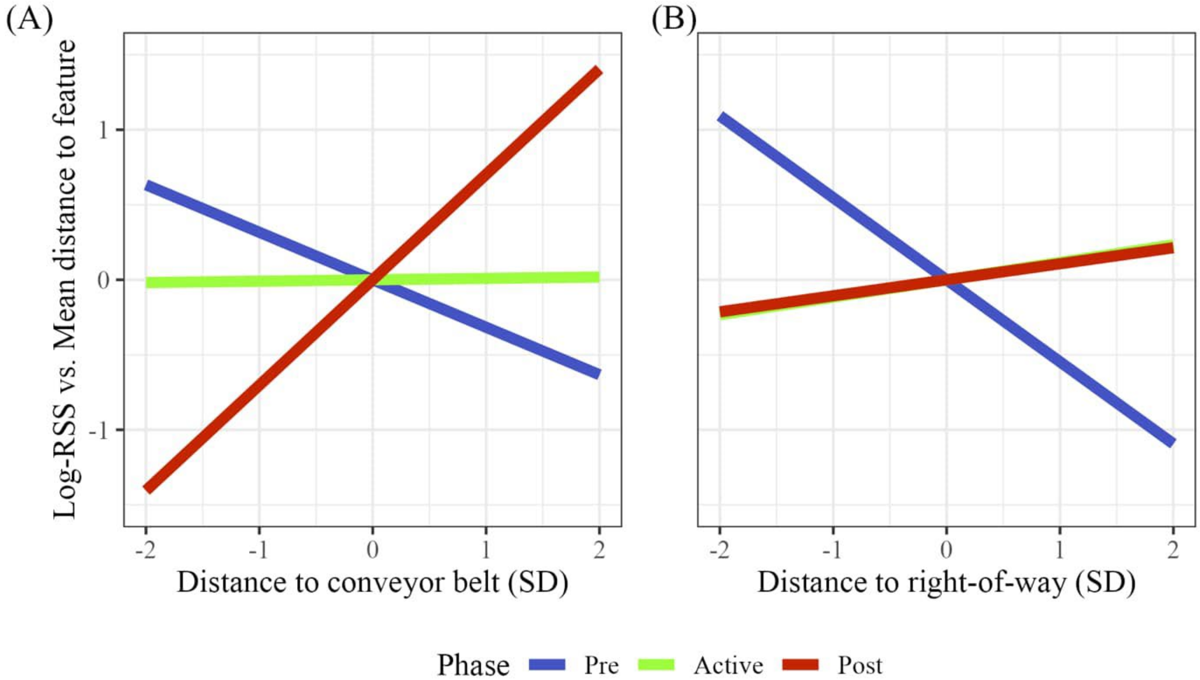

Figure 4. Predictions from generalized mixed-effects models of (A) distance to conveyor belt and (B) distance to right-of-way standardized by one standard deviation (SD) against log relative selection strength (log-RSS) in the pre-, active, and post-construction phases.

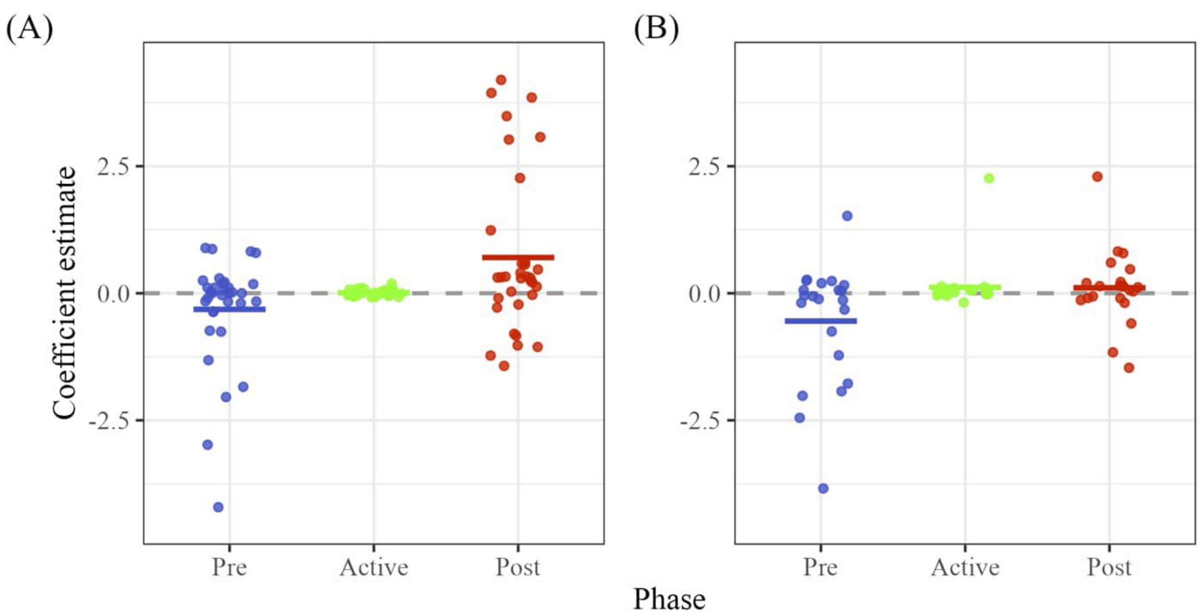

Figure 5. Individual random effects (points) and mean coefficient estimates (lines) from generalized mixed-effects models of standardized (A) distance to conveyor belt and (B) distance to right-of-way in the pre-, active, and post-construction phases.

closer to the conveyor belt in the pre-construction phase and then switched to avoidance post-construction, 31.8% of individuals (7/22) showed avoidance in the pre- and post-construction phases, 27.3% of individuals (6/22) showed selection for closer distance to the conveyor belt in the pre- and post-phases, and 9.1% of individuals (2/22) switched from avoidance in the pre-construction phase to selecting for closer distance in the post-construction phase (Fig. 5). We found that selection for distance to wildlife crossings was not important in any ROW construction phase.

Space-use Patterns

Except for the 1-km distance band for the conveyor belt, the proportion of high-use area declined in the active- and post-construction phases compared to pre-construction for both the conveyor belt (Fig. S1) and ROW (Fig. S2) features within each distance band (Table 4). The largest decline in the proportion of high-use area occurred in the ROW distance bands, with declines of 22.9%–27.3% and 6.3%–12.1% in the active- and post-construction phases respectively, compared to the pre-construction phase (Table 4). Changes in the proportion of high-use area for conveyor belt distance bands were weaker, with declines ranging from 15.2%–19.1% in the 2-km distance band and 4.8%–9.1% in the 3-km distance band in the active and post-construction phases relative to the pre-construction phase (Table 4).

Distance Analysis

Except for the 3-km buffer in the active-construction phase for the conveyor belt, the proportion of locations within distance buffers of the conveyor belt (Fig. 6) and ROW (Fig. 7) declined during active and post-construction relative to pre-construction phases. On average, the proportion of locations in the pre-, active, and post-construction phases for the conveyor belt were 10.3%, 10.2%, and 6.7% at the 1-km buffer, 20.6%, 20.5%, and 16.9% at the 2-km buffer, and 34.6%, 35.6%, and 30.9% at the 3-km buffer, respectively. On average, the proportion of locations in the pre-, active, and post-construction phases for ROW construction were 17.3%,16.2%, and 13.1% at the 1-km buffer, 33.2%, 31.2%, and 25.2% at the 2-km buffer, and 51.8%, 46.0%, and 43.1% at the 3-km buffer, respectively.

Table 4. Total high-use area (km^2) and proportion of high-use area within 3 buffer distances (1-km, 2-km and 3-km) of the conveyor belt (BELT) and right-of-way (ROW) features relative to total area.

Feature	Phase	Total area (km^2)	Proportion in 1-km	Proportion in 2-km	Proportion in 3-km
Belt	Pre	382.8	0.10	0.21	0.33
Belt	Active	409.5	0.08	0.17	0.28
Belt	Post	338.0	0.10	0.20	0.30
ROW	Pre	302.4	0.16	0.33	0.48
ROW	Active	425.7	0.12	0.24	0.37
ROW	Post	316.0	0.15	0.29	0.43

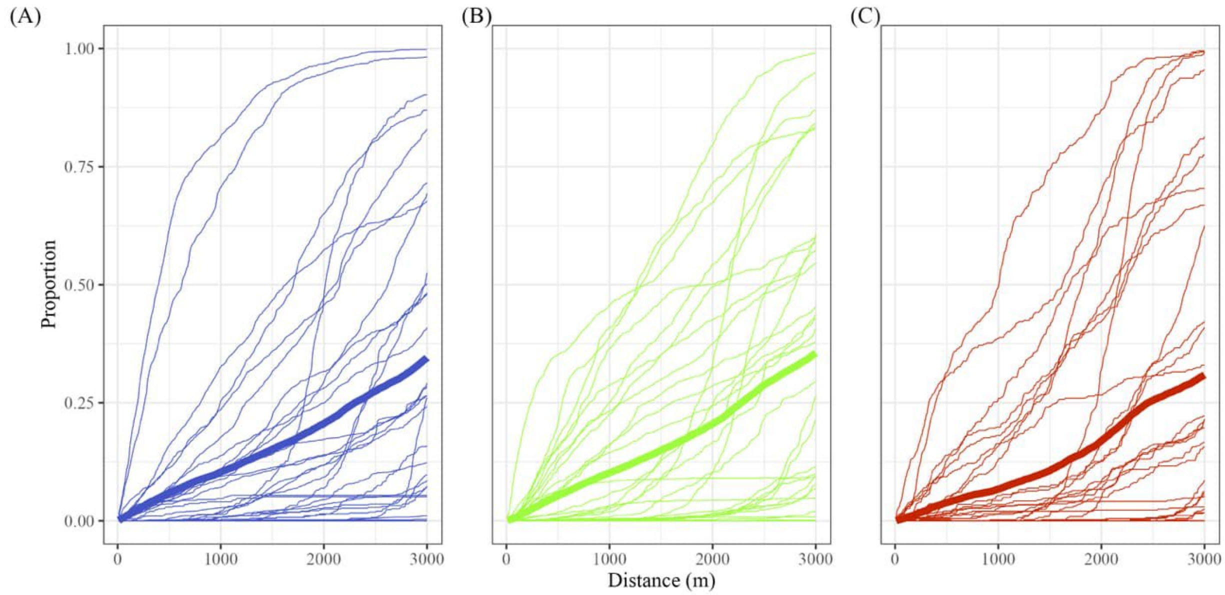

Figure 6. Overall average (thick lines) and individual (thin lines) proportion of locations within 3 km of the conveyor belt in the (A) pre-, (B) active, and (C) post-phases of conveyor belt construction.

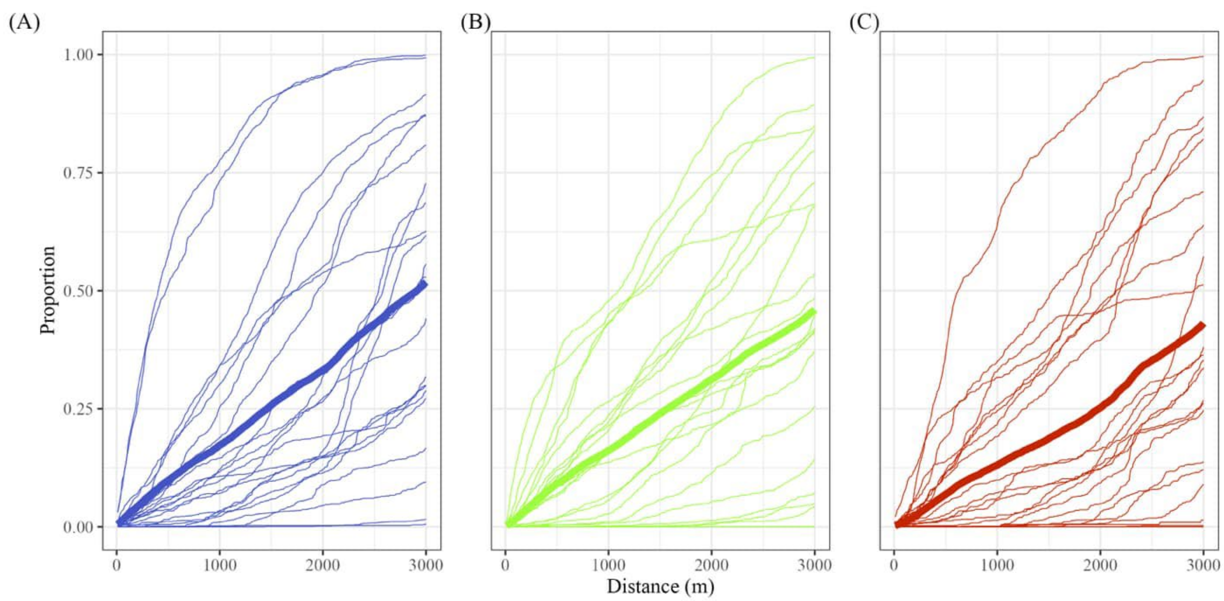

Figure 7. Overall average (thick lines) and individual (thin lines) proportion of locations within 3 km of the right-of-way in the (A) pre- (B) active, and (C) post-phases of right-of-way construction.

We estimated average differences in the minimum distance to the conveyor belt between pre- and post-construction phases of 1,390.8 m (SD = 2,843.2 m) for individuals that changed from negative (i.e., preference) to positive (i.e., avoidance) selection, 554.7 m (SD = 728.4 m) for individuals that changed from positive to negative selection, 915.5 m (SD = 1,432.4 m) for individuals that maintained negative selection, and 255.1 m (SD = 503.5 m) for individuals that maintained positive selection. For the ROW, we estimated average differences in the minimum distance between pre- and post-construction phases of 1,101.3 m (SD = 1,878.0 m) for individuals that changed from negative to positive selection, 29.8 m (SD = 60.9 m) for individuals that changed from positive to negative selection, 442.3 m (SD = 401.1 m) for individuals that maintained negative selection, and 19.0 m (SD = 38.9 m) for individuals that maintained positive selection.

Barrier Behavior Analysis

For our fine-scale analysis, we had 21 adult deer (18 female, 3 male) that had 3-hr GPS fix rates after removing one individual due to poor GPS accuracy. Thus, our data included 137,314 locations spanning 8 March 2022 to 21 February 2025. We determined through sensitivity analysis that the optimal buffer distance was 350 m based on the frequency of quick crosses stabilizing (Fig. S3). In calculating the impermeability index for 50-m conveyor belt segments, we did not include weights based on the number of unique individuals because most sections were encountered by one or two collared individuals, but not necessarily the same individuals, which avoided a downward bias in the impermeability index. Out of 1,776 encounter events, quick cross (42.6%) and bounce (33.3%) events followed by average movements (13.5%), were the most frequent events, while trace (2.2%), back-and-forth (6.9%), and unknown (1.5%) movements occurred at lower frequencies.

Across conveyor belt construction phases, 76.2% of individuals (16/21) in the pre-phase, 47.6% of individuals (10/21) in the active phase, and 53.3% of individuals (8/15) in the post-phase had encounters with the conveyor belt. We found similar rates of normal movement behaviors (i.e., average movement and quick crosses) across pre- (52.8%, SD = 20.0%), active (62.7%, SD = 26.1%), and post-construction (51.0%, SD = 36.1%) phases for the conveyor belt ($F_{2,34}$ = 0.69, P = 0.51; Fig. 8), with a large amount of variation across individuals. Also, altered movement behaviors including back-and-forth, bounce, and trace events were variable across individuals and not statistically different between the pre- (47.2%, SD = 20.0%), active (37.3%, SD = 26.1%), and post-construction (49.0%, SD = 36.1%) phases for the conveyor belt ($F_{2,34}$ = 0.69, P = 0.51; Fig. 8). We found that the impermeability indices were similar between belt construction phases ($F_{2,885}$ = 0.42, P = 0.66), with average values increasing only slightly between the pre- ($\bar{x}$ = 0.42, SD = 0.19) and post-construction ($\bar{x}$ = 0.44, SD = 0.32) phases. However, despite there not being a large difference in the average index scores, there was a substantial reduction in the number of 50-m conveyor belt sections encountered across the pre- (n = 924), active (n = 722), and post-construction (n = 130) phases. The central portion of the conveyor belt where our collared sample occurred experienced reductions in sections encountered, but reductions mainly occurred in the far western portion of the conveyor belt near the sand receiving site in New Mexico (see Fig. S4A–S4C).

Across ROW construction phases, 83.3% of individuals (15/18) in the pre-construction phase, 61.9% of individuals (13/21) in the active phase, and 47.1% of individuals (8/17) in the post-construction phase had encounters with the conveyor belt. We found similar rates of normal movement behaviors (i.e., average movement and quick crosses) across pre- (54.7%, SD = 19.3%), active (47.9%, SD = 23.3%), and post-construction (53.3%, SD = 25.0%) phases of the ROW ($F_{2,35}$ = 0.38, P = 0.69; Fig. 8). Also, altered movement behaviors including back-and-forth, bounce, and trace events were variable across individuals and not statistically different between the pre- (45.3%, SD = 19.3%), active (52.1%, SD = 23.3%), and post-construction (46.7%, SD = 25.0%) phases of the ROW ($F_{2,35}$ = 0.38, P = 0.69; Fig. 8). We found moderate evidence that the impermeability indices were different between ROW construction periods ($F_{2,937}$ = 4.15, P = 0.02), with the differences driven by greater values in the active ($\bar{x}$ = 0.43, SD = 0.20) and post-construction ($\bar{x}$ = 0.44, SD = 0.23) phases compared to the pre-construction ($\bar{x}$ = 0.40, SD = 0.22) phase.

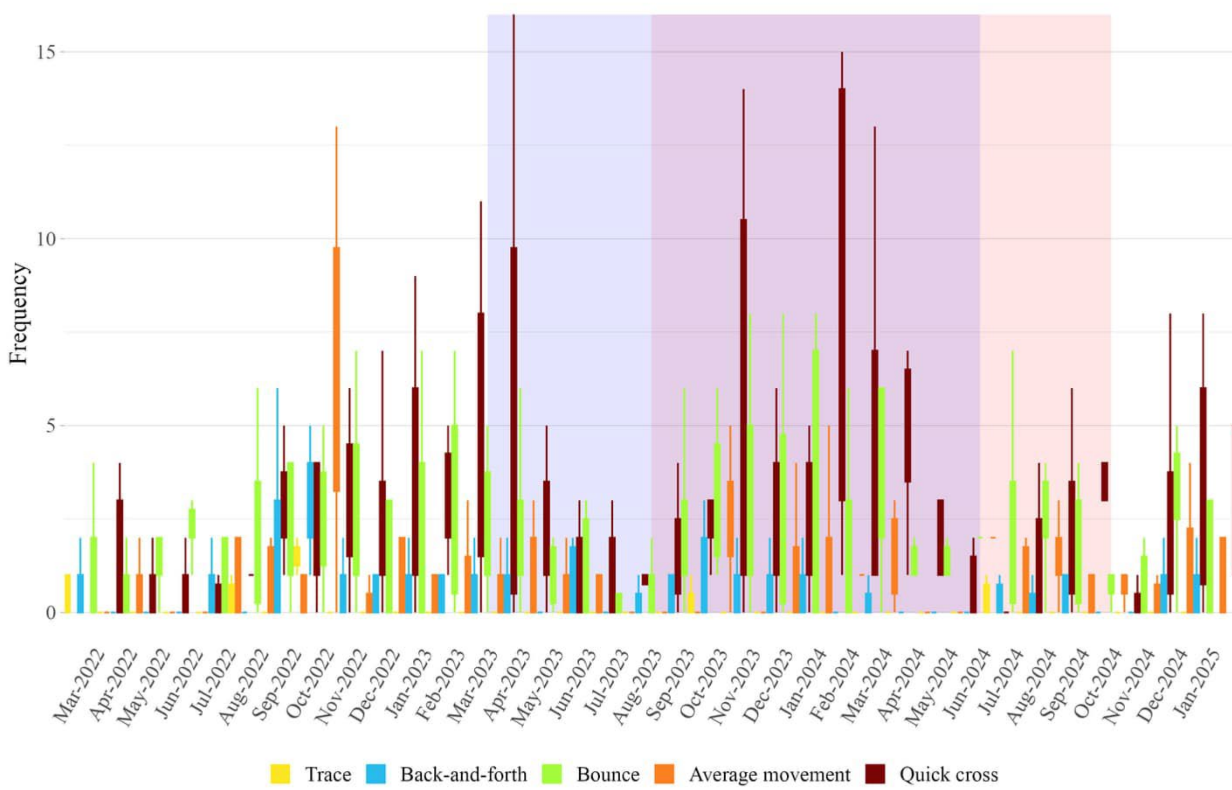

Figure 8. Monthly variability of mule deer barrier behavior including trace, back-and-forth, bounce, average movement, and quick cross frequencies. Note that active construction phases of the right-of-way (blue shading) and for the conveyor belt (red shading) with the purple shading indicating both features in active construction.

We found that most wildlife crossings had impermeability indices that varied across conveyor belt and ROW construction phases, with some crossings becoming more permeable while others became less permeable. About 85.7% and 71.4% of wildlife crossings that were encountered in the pre-construction phase were not encountered in the post-construction phase for the conveyor belt and ROW, respectively. For wildlife crossings that continued to have encounters in the post-construction phase, we found that most had low to moderate values of impermeability (i.e., 0.15 to 0.67) with none being highly impermeable (i.e., 0.80–1.00). We were only able to estimate index values for a subset of wildlife crossings as some were outside of the range of our GPS dataset for this analysis (see Table S4).

Discussion

Decomposing the potential impacts of energy infrastructure on wildlife populations is imperative for effective management and mitigation for species conservation. In our study, we found significant post-construction impacts of the Kermit conveyor belt on mule deer habitat selection, space use, and movement. We detected avoidance of the conveyor belt after construction was completed in our 3rd-order habitat selection analysis, with nearly 70% of individuals showing avoidance and a significant average effect across the population. As predicted, we found more attenuated responses to ROW construction with about 64% of individuals showing weak avoidance after construction was completed. Space-use and distance analyses demonstrated that deer utilized areas close to the conveyor belt less in the post-construction phases for the conveyor belt and ROW compared to pre-construction. Consistent with this observed decline in proximity to the conveyor belt, our barrier behavior analysis detected a substantial decline in conveyor belt encounters in the post-construction phase, with the western section of the conveyor belt near the sand receiving facility in New Mexico experiencing the largest declines. We found that barrier behavior events did not change significantly over construction phases, with relatively consistent normal and altered behavior over the study, and relatively high variation in the permeability of wildlife crossing locations that were used by our sample of collared animals.

Habitat selection analysis provides a means to evaluate how animals respond to environmental disturbance. We accounted for a set of base and human disturbance covariates beyond evaluating deer responses to the conveyor belt and ROW. Previous mule deer studies found that elevation (Sawyer et al. 2006, 2009; Northrup et al. 2015, Sorensen et al. 2020) and distance to water (Sorensen et al. 2020, Bird et al. 2024) were important predictors for deer habitat selection, while we found that elevation was not important for habitat selection and that deer only selected for closer distance to water in the monsoon and spring seasons. These results were intuitive because our study area had little variation in elevation (i.e., a change of 260 m) and the availability of water may be less predictable in this arid environment outside of the late spring and monsoon seasons when little rainfall occurs. While most habitat selection studies that focused on energy development did not account for forage availability (e.g., Sawyer et al. 2006, Northrup et al. 2015), we found that SAVI was an important predictor for both conveyor belt and

ROW analyses and highly predictive of mule deer habitat selection where greater vegetative productivity was selected for. Also, consistent with previous results (Northrup et al. 2015), we found that selection for distance to roads depended on the time of day, with strong avoidance for roads in the day when most human activity occurs. Selection for distance to oil and gas wells was weaker compared to roads but deer did avoid oil and gas wells in the daytime in our conveyor belt analysis. However, we did not differentiate between active drilling and production phases of oil and gas wells as in other studies (Sawyer et al. 2009, Northrup et al. 2015), mainly because our primary focus was on the conveyor belt and ROW features. Certainly, we might assume that deer would show more avoidance of active drilling of oil and gas wells compared to the production phase as others found, which increases disturbance due to human activity, noise and traffic around the active well sites (Northrup et al. 2021). Importantly, our 3rd-order habitat selection analysis provided evidence that on average, the population avoided the conveyor belt post-construction compared to pre- and active construction phases. Mule deer could be repelled by the noise created by the operation of the conveyor belt. For instance, Kleist et al. (2021) found evidence that mule deer were detected less frequently at gas well sites and associated roads with greater levels of daily anthropogenic noise. In our study it appears that even those individuals that selected to be closer to the conveyor belt after construction still showed fine-scale avoidance for the belt (e.g., Fig. 2D–F). Indeed, our analysis of these individuals found that the average difference in minimum distances from the conveyor belt route increased by 555–915 m between the pre- and post-construction phases, which aligns with fine-scale avoidance responses from previous studies (Northup et al. 2015, Sawyer et al. 2017). Thus, fine-scale avoidance effects are important to account for along with 3rd-order habitat selection analyses.

Our analysis of fine-scale responses to the conveyor belt and ROW construction included space use, distance, and barrier behavior analyses. First, we found that the proportion of high use area declined in active and post-construction phases compared to the pre-construction phase for both features by factors of 4.8%–27.3%. Sawyer et al. (2025) found that pronghorn (*Antilocapra americana*) proportion of high-use habitat decreased by 40–60% in response to utility-scale solar energy development. The lower response of mule deer to the conveyor belt compared to pronghorn to the utility-scale solar energy development could relate to difference in species sensitivity to disturbance or due to the habitat constraints on the landscape. A recent study found that pronghorn were more sensitive to fences compared to mule deer, with mule deer more likely to maintain average movement and less likely to exhibit bounce behavior compared to pronghorn (Xu et al. 2021). In addition, mule deer in our study area were already exposed to high levels of human activity and habitat disturbances due to oil field construction and production activities, and thus they could have developed some level of habituation to human activity. Consistently, we found that the proportion of locations declined over conveyor belt and ROW construction, with the greatest effects occurring within 1-km at a 24% to 35% decline on average. Our results were comparable to Sawyer et al. (2025), which found that 10% of all pronghorn locations were within 0.75 km and 1.70 km of the utility-scale solar energy development before and after construction, respectively. In our study, 10% of mule deer locations were within 0.97 km and

1.43 km on average of the conveyor belt in the pre- and post-construction phases, respectively. Finally, our barrier behavior analysis did not detect a change in normal or altered behaviors over the study period but did highlight a substantial reduction in encounter events across large sections of the conveyor belt after construction was completed along with reductions in permeability in some sections. Although we cannot assume that no crossing events were attempted in these sections, the evidence of fine-scale avoidance of the conveyor belt suggests this was likely the case, especially the western section near the sand receiving facility in New Mexico where the effect on deer movements was most pronounced. Consistently, our RSF analyses found no evidence that deer selected for closer distance to wildlife crossing structures in any construction phase.

Like any study, there are a few caveats to our results. Due to a delay in the completion of the conveyor belt, our post-construction phase only included 4 months of GPS data. Despite this limitation, our sample size of GPS-collared deer that were on-air over the three phases of construction (pre-, active, and post-) exceeded sample sizes previously used to investigate the response of ungulates to other energy infrastructure developments (e.g., Sawyer et al. 2025). Our sample sizes of individuals with 3-hr fix rates were lower because of the need to adjust our transmission rate to every other fix to account for the high cost of uploading GPS data to the Iridium satellite network. Nonetheless, we had 21 individual deer with 3-hr fix rates for our barrier behavior analysis, which was comparable to other studies that performed similar analyses (e.g., Xu et al. 2021). In our inference to wildlife crossings, it is important to note that we did not monitor crossing rates on the ground (e.g., with game cameras) to determine the use or permeability of these structures. Rather, we used the closest 50-m segment of conveyor belt to each wildlife crossing in our barrier behavior analysis to investigate encounter rates and permeability at these structures. Finally, our GPS data only spanned two-thirds of the conveyor belt including the western and central portions, and thus we could not provide inference to 42% of the wildlife crossings.

In our multi-scale analysis, we demonstrated negative impacts of the conveyor belt on mule deer, but due to relatively short duration of post-construction data in our study, it is unclear if deer will become habituated to the conveyor belt over time and be less affected as far as avoidance of the belt and reduced crossing behavior—previous research suggests that mule deer may not habituate to oil and gas infrastructure and avoidance behavior could persist into the future (e.g., Sawyer et al. 2017). On one hand, the conveyor belt will reduce truck traffic on congested roads that deer showed strong avoidance for in our study in the daytime but could potentially increase future drilling in the region due to the ease of providing sand, which could be to the detriment of deer populations in the region (Cortez and Lathan 2025). The direct and indirect loss of mule deer habitat in the area from oil and gas well sites and roads combined with the conveyor belt will need to be addressed through careful monitoring of wildlife crossing structures to ensure that deer movement corridors are conserved in the future in this region. It appears that less than a third of the wildlife crossings structures used by our GPS-collared deer in the study were used after completion of the conveyor belt. Use of camera traps to monitor these crossing structures could help document use by mule deer and other sensitive species in the region. Characteristics at crossing structures could also to be evaluated to explain variation in use across wildlife species along the length of the conveyor belt.

Because this region is relatively flat, deer will not have the rugged topography that can mediate avoidance behavior. The impacts to mule deer populations in this region from the rapid growth of energy developments may take years to realize in terms of abundance, but research from other regions that underwent similar oil and gas booms suggest that declines in deer abundance may be expected. Thus, cooperation between state, federal, private landowners, and industry partners will be important to successfully conserve mule deer and other sensitive species in the region and mitigate the potential negative impacts of future energy developments.

Acknowledgements

We thank the Bureau of Land Management, Carlsbad Field Office, and New Mexico Department of Game and Fish for logistical support. C. Stallings, W. Livingston, H. C. Cushman, O. Duvuvuei, L. Vanlandingham, N. Riso, C. Smith and C. Squires captured study animals. Additional field and data assistance was provided by R. Francis, A. Jolliff, M. Keeling, and J. Nierman. Data are available on reasonable request. Funding for this project was provided by Atlas Sand Company, LLC. Any use of trade, firm, or product names is for descriptive purposes only and does not imply endorsement by the U.S. Government.

Literature Cited

Allred, B. W., W. K. Smith, D. Twidwell, J. H. Haggerty, S. W. Running, D. E. Naugle, and S. D. Fuhlendort. 2015. Ecosystem services lost to oil and gas in North America. Science 348: 401–402.

Aristizabal, J. F., N. Y. Almanza-Ortiz, C. Vital-Garcia, N. Righini, and M. P. Olivas-Sanchez. 2026. The seasonal diet selection and nutritional niche of mule deer in a Chihuahuan semi-desert. Wild 3:1–16.

Bird, D. E., L. E. D'Acunto, D. Ginter, G. Harper, and P. A. Zollner. 2024. Temporal habitat use of mule deer in the Pueblo of Santa Ana, New Mexico. The Journal of Wildlife Management 88:e22621.

Bivand R, and S. Luque S. 2025. suntools: Calculate Sun Position, Sunrise, Sunset, Solar Noon and Twilight. R package version 1.1.0. <https://CRAN.R-project.org/package=suntools>.

Boyce, M. S., P. R. Vernier, S. E. Nielsen, and F. K. A. Schmiegelow. 2002. Evaluating resources selection functions. Ecological Modeling. 157:281–300.

Brooks, M. E., K. Kristensen, K. J. van Benthem, A. Magnusson, C. W. Berg, A. Nielsen, J. J. Skaug, M. Machler, and B. M. Bolker. 2017. glmmTMB Balances speed and flexibility among packages for zero-inflated generalized linear mixed modeling. The R Journal 9:378–400.

Charlebois, M. L., H. G. Skatter, and J. L. Kansas. 2023. Influence of aboveground pipeline and associated factors on movement of winter-active boreal mammals in the Alberta in-situ oil sands. Northwest Science 96:80–93.

Cook, T. J. Perrin, and D. V. Wagener. 2018. Hydraulically fractured horizontal wells account for most new oil and natural gas wells. United States Energy Information Administration. < see https://www.eia.gov/todayinenergy/detail.php?id=34732>. Accessed 2 Feb 2026.

Cortez, J., and N. Lathan. 2025. This 'Dune' isn't fiction. It's the longest conveyor belt in the US and moving sand in Texas. The Seattle Times. <see https://www.seattletimes.com/business/this-dune-isnt-fiction-its-the-longest-conveyer-belt-in-the-us-and-moving-sand-in-texas/> . Accessed 15 Oct 2025.

Dormann, C. F., J. Elith, S. Bacher, C. Buchmann, G. Carl, G. Carré, J. R. García Marquéz, B. Gruber, B. Lafourcade, P, J. Leitão, T. Münkemüller, C. McClean, P. E. Osborne, B. Reineking, B. Schröder, A. K Skidmore, D. Zurell, and S. Lautenback. 2013. Collinearity: a review of methods to deal with it and a simulation study evaluating their performance. Ecography 36:27–46.

Dunne, B. M., and M. S. Quinn. 2009. Effectiveness of above-ground pipeline mitigation for moose (*Alces alces*) and other large mammals. Biological Conservation 142:332–343.

Dwinnell, S. P. H., H. Sawyer, J. E. Randall, J. L. Beck, J. S. Forbey, G. L. Fralick, and K. L. Monteith. 2019. Where to forage when afraid: Does perceived risk impair use of the foodscape? Ecological Applications 29:e01972.

Golding, G., D. Morales-Burnett, and K. Patel. 2025. New Mexico fuels U.S. crude oil output, function for local programs. Federal Reserve Bank of Dallas. <see https://www.dallasfed.org/research/swe/2025/swe2504#:~:text=New%20Mexico%20has%20become%20a,state%20coffers%20in%20the%20process>. Accessed 23 Oct 2025.

Gillies, C. S., M. Hebblewhite, S. E. Nielsen, M. A. Krawchuk, C. L. Aldridge, J. L. Frair, D. J. Saher, C. E. Stevens, and C. L. Jerde. 2006. Application of random effects to the study of resource selection by animals. Journal of Animal Ecology 75:887–898.

Google. 2025. Google Compute Engine: a computing and hosting service. Google Cloud. < https://cloud.google.com/products/compute>. Accessed 1 Sep 2025.

Griffith, G. E., S. A. Bryce, J. M. Omernik, J. A. Comstock, A. C. Rogers, B. Harrison, S. L. Hatch, and D. Bezanson. 2004. Ecoregions of Texas (color poster with map, descriptive text, and photographs): Reston, Virginia, U.S. Geological Survey (map scale 1:2,500,000).

Griffith, G. E., J. M. Omernik, M. M. McGraw, G. Z. Jacobi, C. M. Canavan, T. S. Schrader, D. Mercer, R. Hill, and B. C. Moran. 2006). Ecoregions of New Mexico (map). U.S. Geological Survey.

Harrity, E. J., M. Traphagen, M. Bethel, A. N. Facka, M. Dax, and E. Burns. 2024. USA-Mexico border wall impedes wildlife movement. Frontiers in Ecology and Evolution 12:1487911.

Hebblewhite, M. 2017. Billion dollar boreal woodland caribou and the biodiversity impacts of the global oil and gas industry. Biological Conservation 206:102–111.

Hosmer, D.W., and S. Lemeshow. 2000. Applied logistic regression. John Wiley and Sons, New York.

Hurley, M. A., M. Hebblewhite, P. M. Lukacs, J. J. Nowak, J. M. Gaillard, and C. Bonenfant. 2017. Regional-scale models for predicting overwinter survival of juvenile ungulates. Journal of Wildlife Management 81:364–378.

Johnson, D.H., 1980. The comparison of usage and availability measurements for evaluating resource preference. Ecology 61:65–71.

Jung, T. S., T. M Hegel, T. W. Bentzen, K. Egli, L. Jessup, M. Kienzler, K. Kuba, P. M. Kukka, K. Russell, M. P Suitor, and K. Tatumi. 2018. Accuarcy and performance of low-feature GPS collars deployed on bison *Bison bison* and caribou *Rangifer tarandus*. Wildlife Biology 1:wlb.00404.

Kleist, N. J., R. R. Buxton, P. E. Lendrum, C. Linares, K. R. Crooks, and G. Wittemyer. 2021. Noise and landscape features influence habitat use of mammalian herbivores in a natural gas field. Journal of Animal Ecology 90:875–885.

Kranstauber, B, R. Kays, S. D. LaPoint, M. Wikelski, and K. Safi. 2012. A dynamics Brownian bridge movement model to estimate utilization distributions for heterogeneous animal movement. Journal of Animal Ecology 81:738–746.

Kranstauber, B, M. Smolla, and A. Scharf. 2024. move: Visualizing and analyzing animal track data. R package version 4.2.6. <https://CRAN.R-project.org/package=move>.

Lovelace, R., and R. Ellison .2018. stplanr: A package for transport planning. The R Journal 10:10. <https://doi.org/10.32614/RJ-2018-053>.

Lovich, J. E., and J. R. Ennen. 2011. Wildlife conservation and solar energy development in the desert southwest, United States. Bioscience 61:982–992.

Manly, B. F. J., L. L. McDonald, D. L Thomas, R. L. McDonald, and W. P. Erickson. 2002. Resource selection by animals: statistical design and analysis for field studies, 2nd edn. Kluwer. Academic Publishers, Dordrecht.

Muff, S., J. Signer, and J. Fieberg. 2019. Accounting for individual-specific variation in habitat-selection studies: efficient estimation of mixed-effects models using Bayesian or frequentist computation. Journal of Animal Ecology. 89:80–92.

NASA. 2022. World's longest conveyor belt system. NASA Earth Observatory. <https://science.nasa.gov/earth/earth-observatory/worlds-longest-conveyor-belt-system-150869/>. Accessed 21 Oct 2025.

NASA JPL. 2021. NASADEM Merged DEM Global 1 arc second V001. Distributed by OpenTopography. <https://doi.org/10.5069/G93T9FD9>. Accessed 21 Jan 2026.

Northrup, J. M., C. R. Anderson Jr., and G. Wittemyer. 2015. Quantifying spatial habitat loss from hydrocarbon development through assessing habitat selection patterns of mule deer. Global Change Biology 21:3961–3970.

Northrup, J. M., C. R. Anderson Jr., B. D. Gerber, and G. Wittemyer. 2021. Behavior and demographic responses of mule deer to energy development on winter range. Wildlife Monographs 208:1–37.

Pebesma, E., 2018. Simple Features for R: standardized support for spatial vector data. The R Journal 10: 439-446.

Pebesma, E., and R. Bivand. 2023. Spatial data science: with applications in R. Chapman and Hall/CRC, Boca Raton, Florida.

Peterson, R. S., and C. S. Boyd. 1998. Ecology and management of sand shinnery oak communities: a literature review. RMRS GTR-16. United States Department of Agriculture, Forest Service, Rocky Mountain Experiment Station, Fort Collins, Colorado.

QGIS Development Team. 2025. QGIS Geographic Information System. Available online: <http://qgis.org>. Accessed on 15 Mar 2025.

R Core Team. 2025. R: A language and environment for statistical computing. R Foundation for Statistical Computing, Vienna, Austria. https://www.R-project.org/.

Robb, B. S., J. A. Merkle, J. Sawyer, J. L. Beck, and M. J. Kauffman. 2022. Nowhere to run: pronghorn space use impacted by semi-permeability of barriers. Journal of Wildlife Management 86:e22212.

Rutherford, T. K., L. M. Maxwell, N. J. Kleist, E. C. Teige, R. J. Lehrter, M. A. Gilbert, D. J. A. Wood, A. N. Johnston, C. Mengelt, J. C. Tull, T. S. Haby, and S. K. Carter. 2023. Effects of noise from oil and gas development on ungulates and small mammals—A science synthesis to inform National Environmental Policy Act analyses (ver. 1.1, July 2024): U.S. Geological Survey Scientific Investigations Report 2023–5114, 44 p., <https://doi.org/10.3133/https://doi.org/10.3133/sir20235114>.

Sawyer, H., M. J. Kauffman, and R. M. Nielson. 2009. Influence of well pad activity on winter habitat selection patterns of mule deer. Journal of Wildlife Management 73:1052–1061.

Sawyer, H., N. M. Korfanta, R. M. Nielson, K. L. Monteith, and D. Strickland. 2017. Mule deer and energy development—long term trends of habituation and abundance. Global Change Biology 23:4521–4529.

Sawyer, H., J. A. Merkle, A. D. Middleton, S. P. H. Dwinnell, and K. Monteith. 2019. Migratory plasticity is not ubiquitous among large herbivores. Journal of Animal Ecology 88:450–460.

Sawyer, H., R. M. Nielson, F. G. Lindzey, and L. L. McDonald. 2006. Winter habitat selection of mule deer before and during development of a natural gas field. Journal of Wildlife Management 70:396–403.

Sawyer, H. K. T. Smith, B. S. Robb, and J. A. Merkle. 2025. Ungulate use before and after utility-scale solar development. Ecological Solutions and Evidence 6:e70071.

Schuyler, E. M., K. M. Dugger, and D. H. Jackson. 2019. Effects of distribution, behavior, and climate on mule deer survival. Journal of Wildlife Management 83:89–99.

Schwarz, G. 1978. Estimating the dimension of a model. Annals of Statistics 6:461–464.

Shanley, C. S., D. R. Eacker, C. P. Reynolds, B. M. B. Bennetsen, and S. L. Gilbert. 2021. Using LiDAR and random forest to improve deer habitat models in a managed forest landscape. Forest Ecology and Management 499:119580.

Sikaria H., S. Arora, A. Tandon, and K. Kathuria. 2026. rLandsat: Landsat data complete download process. R package version 0.1.1. <https://github.com/atlanhq/rLandsat>.

Signer J, J. Fieberg, T. Avgar. 2019. Animal movement tools (amt): R package for managing tracking data and conducting habitat selection analyses. Ecology and Evolution 9:880–890.

Skelly, B. P., C. T. Rota, J. L. Kolar, B. A. Stillings, J. W. Edwards, M. A. Foster, R. M Williamson, and J. J. Millspaugh. 2024. Mule deer mortality in the northern Great Plains in a landscape altered by oil and natural gas extraction. Journal of Wildlife Management 88:e22619.

Sorensen, G. E., Kramer, D. W., J. W. Cain III, C. A. Taylor, P. S. Gipson, M. C. Wallace, R. D. Cox, and W. B. Ballard. 2020. Mule deer habitat selection following vegetation thinning treatments in New Mexico. Wildlife Society Bulletin 44:122–129.

USGS. 2025. Landsat soil adjusted vegetation index. United States Geological Survey. <https://www.usgs.gov/landsat-missions/landsat-soil-adjusted-vegetation-index>. Accessed 10 Jun 2025.

Villarreal, M. L., J. Pierce, E. K. Waller, S. N. Chambers, M. C. Duniway, T. Fancher, M. T. Hannon, G. A. Montgomery, K. Rexer, J. Simonsen, A. J. Titolo, and R. Uncapher. 2023. Geodatabase of oil and gas pads and roads within the Bureau of Land Management's Carlsbad Field Office administrative boundary, New Mexico: U.S. Geological Survey data release, <https://doi.org/10.5066/P9GKIPLH>.

Xu W., and V. Herrmann. 2026. BaBA: Barrier behavior analysis (BaBA). R package version 2.1. <https://github.com/wx-ecology/BaBA>.

Xu W., N. Dejid, V. Herrmann, H. Sawyer, and A. D. Middleton. 2021. Barrier behavior analysis (BaBA) reveals extensive effects of fencing on wide-ranging ungulates. Journal of Applied Ecology 58:690–698.

Appendix

Table S1. Summary of covariates considered in habitat selection analysis including variable description, category, mean ($\bar{x}$) and standard deviation (SD), and range for used and available locations. Note that values are based on used GPS locations to assess the effects of distance to conveyor belt.

Variable description	Category	Used $\bar{x}$ (SD)	Used Range	Available $\bar{x}$ (SD)	Available Range
Elevation (m)	Base	994.2 (42.1)	841.2 to 1,095.2	995.1 (42.7)	880.6 to 1,091.0
Soil Adjusted Vegetation Index	Base	0.13 (0.01)	−0.01 to 0.19	0.13 (0.01)	−0.35 to 0.22
Shrub cover (%) between 0.5–2.0 m	Base	0.29 (0.14)	0.00 to 0.56	0.30 (0.13)	0.00 to 0.57
Distance to water (m)	Base	1,693.2 (1,470.2)	0.01 to 7,709.8	1,816.3 (1,513.8)	0.00 to 7,425.3
Distance to road (m)	Human disturbance	459.5 (362.3)	0.01 to 2,466.4	412.2 (365.8)	0.00 to 2,481.4
Distance to oil or gas well (m)	Human disturbance	443.0 (254.4)	0.42 to 1,588.0	414.5 (269.1)	0.53 to 1,688.5
Distance to right-of-way (m)	Treatment	6,317.2 (7,894.3)	0.00 to 70,783.1	6,507.4 (7,938.0)	0.00 to 72,396.7
Distance to conveyor belt (m)	Treatment	8,286.9 (11,710.3)	0.01 to 70,916.3	8,466.9 (11,532.4)	0.00 to 72,254.7
Distance to wildlife crossing (m)	Treatment	4,873.3 (3,247.1)	6.5 to 24,994.1	5,097.4 (3,424.9)	9.6 to 17,182.2

Table S2. Model selection results for conveyor belt including model number (M_k) and formula, Bayesian Information Criteria (BIC), log-likelihood (LL), residual degrees of freedom (DF_{resid}), and average Spearman's correlation coefficient ($\bar{\rho}$) from k-fold cross-validation routine. We compared 30 models that included the following covariates: elevation in meters (elev_m), Soil-adjusted Vegetation Index (savi), percent vegetation cover between 0.5–2.0 m (veg_c), distance to water in meters (wtr_ds), distance to oil and gas wells in meters (wll_ds), distance to roads in meters (rd_dst), distance to conveyor belt in meters (blt_ds), and distance to wildlife crossing in meters (crssn). Additionally, we included interaction terms for the following factors: day or night (dy_nght), season (winter, spring, monsoon, and rut), and the phase of conveyor belt construction (blt_stg). Note that that interactions terms were included without the main effects of covariate/factors because the factors had no biological meaning as main effects and were only used to stratify the covariate effects.

M_k	Model formula	BIC	LL	DF_{resid}	$\bar{\rho}$
27	~base+rd_dst:dy_nght+wll_ds:dy_nght+blt_ds:blt_stg	451318347	−225658859	656641	0.993
28	~base+rd_dst:dy_nght+wll_ds:dy_nght+blt_ds:dy_nght:blt_stg	451203026	−225601078	656623	0.988
30	~base+rd_dst:dy_nght+wll_ds:dy_nght+crssn:dy_nght:blt_stg	449619660	−224809394	656623	0.976
29	~base+rd_dst:dy_nght+wll_ds:dy_nght+crssn:blt_stg	449891293	−224945332	656641	0.973
26	~base+rd_dst:dy_nght+wll_ds:dy_nght	455542868	−227771179	656650	0.971
23	~base+wll_ds:dy_nght	460530470	−230265014	656655	0.954
19	~base+rd_dst:dy_nght	457720235	−228859896	656655	0.937
25	~base+wll_ds:dy_nght:season	459516243	−229757639	656616	0.937
8	~savi:dy_nght:season	479780105	−239889744	656642	0.935
6	~savi:dy_nght	481198793	−240599350	656681	0.932
7	~savi:season	480518486	−240259136	656672	0.922
24	~base+wll_ds:season	460912038	−230455738	656646	0.920
5	~savi	481797010	−240898478	656684	0.918
20	~base+rd_dst:season	458360532	−229179985	656646	0.905
21	~base+rd_dst:season:dy_nght	456445326	−228222181	656616	0.905
22	~base+wll_ds	461729460	−230864529	656658	0.905
18	~base+rd_dst	459450394	−229724996	656658	0.893
17	~base	464233362	−232116493	656660	0.879
15	~wtr_ds:season	483667788	−241833787	656672	0.372
16	~wtr_ds:dy_nght:season	483394448	−241696916	656642	0.371
10	~veg_c:dy_nght	490628995	−245314451	656681	0.351
9	~veg_c	491036584	−245518265	656684	0.317
12	~veg_c:dy_nght:season	489869467	−244934426	656642	0.302
14	~wtr_ds:dy_nght	487275077	−243637491	656681	0.229
13	~ wtr_ds	487443712	−243721829	656684	0.215
11	~veg_c:season	490416064	−245207925	656672	0.006
4	~elev_m:dy_nght:season	485105650	−242552517	656642	−0.256
3	~elev_m:season	485185370	−242592578	656672	−0.295
1	~elev_m	486976010	−243487978	656684	−0.402
2	~elev_m:dy_nght	486921615	−243460760	656681	−0.404

[1]Note that the formula for the base model for conveyor belt model selection was: elev_m+savi:dy_nght+veg_c:dy_nght+wtr_ds:season.

Table S3. Model selection results for the right-of-way including model number (M_k) and formula, Bayesian Information Criteria (BIC), log-likelihood (LL), residual degrees of freedom (DF_{resid}), and average Spearman's correlation coefficient ($\bar{\rho}$) from k-fold cross-validation routine. We compared 30 models that included the following covariates: elevation in meters (elev_m), Soil-adjusted Vegetation Index (savi), percent vegetation cover between 0.5–2.0 m (veg_c), distance to water in meters (wtr_ds), distance to oil and gas wells in meters (wll_ds), distance to roads in meters (rd_dst), distance to right-of-way in meters (bw_dst), and distance to wildlife crossing in meters (crssn). Additionally, we included interaction terms for the following factors: day or night (dy_nght), season (winter, spring, monsoon, and rut), and the phase of right-of-way construction (row_stg). Note that that interactions terms were included without the main effects of covariate/factors because the factors had no biological meaning as main effects and were only used to stratify the covariate effects.

M_k	Model formula	BIC	LL	DF_{resid}	$\bar{\rho}$
6	~savi:dy_nght	368753776	−184376842	503201	0.964
5	~savi	369117683	−184558815	503204	0.954
7	~savi:season	368409080	−184204435	503192	0.954
8	~savi:dy_nght:season	367941508	−183970452	503162	0.952
19	~base+rd_dst:dy_nght	352964014	−176481712	503163	0.944
29	~base+rd_dst:dy_nght+wll_ds:dy_nght+crssn:row_stg	346410884	−173205133	503161	0.930
27	~base+rd_dst:dy_nght+wll_ds:dy_nght+rw_dst:row_stg	347267962	−173633672	503161	0.922
28	~base+rd_dst:dy_nght+wll_ds:dy_nght+rw_dst:dy_nght:row_stg	347116553	−173557850	503143	0.922
30	~base+rd_dst:dy_nght+wll_ds:dy_nght+crssn:dy_nght:row_stg	346151373	−173075260	503143	0.922
18	~base+rd_dst	354052337	−177025893	503166	0.898
20	~base+rd_dst:season	353264849	−176632070	503154	0.886
21	~base+rd_dst:season:dy_nght	351993435	−175996166	503124	0.886
26	~base+rd_dst:dy_nght+wll_ds:dy_nght	351104960	−175552152	503158	0.872
23	~base+wll_ds:dy_nght	353948277	−176973843	503163	0.852
25	~base+wll_ds:dy_nght:season	353176797	−176587847	503124	0.850
17	~base	356304718	−178152096	503168	0.845
22	~base+wll_ds	354850754	−177425101	503166	0.845
24	~base+wll_ds:season	354254480	−177126885	503154	0.827
15	~wtr_ds:season	370898005	−185448897	503192	0.377
16	~wtr_ds:dy_nght:season	370631565	−185315480	503162	0.353
13	~ wtr_ds	374294643	−187147295	503204	0.345
14	~wtr_ds:dy_nght	374130037	−187064972	503201	0.336
2	~elev_m:dy_nght	373735464	−186867686	503201	0.152
1	~elev_m	373763088	−186881518	503204	0.113
4	~elev_m:dy_nght:season	372342542	−186170969	503162	0.113
11	~veg_c:season	376457154	−188228472	503192	0.103
10	~veg_c:dy_nght	376651401	−188325655	503201	0.096
12	~veg_c:dy_nght:season	376058092	−188028744	503162	0.069
3	~elev_m:season	372405954	−186202872	503192	0.038
9	~veg_c	376922003	−188460975	503204	0.002

[1]Note that the formula for the base model for right-of-way model selection was: elev_m:dy_nght+savi:dy_nght +veg_c:season+wtr_ds:season

Table S4. Locations of wildlife crossings along the conveyor belt and impermeability indices for encounter events from barrier behavior analysis. Note that blank values indicate the wildlife crossing did not have any encounter events classified at the nearest 50-m section of conveyor belt and 0 and 1 represent the lowest and highest impermeability, respectively.

Longitude	Latitude	Overall	Pre Belt	Active Belt	Post Belt	Pre Right-of-way	Active Right-of-way	Post Right-of-way
−103.6216750	32.03194997	0.44	0.44	-	-	0.44	-	-
−103.5513139	32.00847102	-	-	-	-	-	-	-
−103.5908026	32.01299505	0.40	0.33	1.00	-	0.11	0.62	-
−103.6084052	32.02176404	0.60	0.60	-	-	0.60	-	-
−103.6522179	32.04743885	-	-	-	-	-	-	-
−103.6601968	32.05077494	0.43	0.43	-	-	0.00	0.75	-
−103.6732381	32.05528612	-	-	-	-	-	-	-
−103.6870508	32.05804894	-	-	-	-	-	-	-
−103.0842675	31.98928100	-	-	-	-	-	-	-
−103.0919242	31.99113227	-	-	-	-	-	-	-
−103.1233804	31.99659985	-	-	-	-	-	-	-
−103.1483477	31.99604279	-	-	-	-	-	-	-
−103.1730752	31.99849890	-	-	-	-	-	-	-
−103.1625780	31.99711795	-	-	-	-	-	-	-
−103.3176564	31.99968472	0.48	0.57	0.17	-	0.55	0.29	-
−103.1831254	31.99952465	-	-	-	-	-	-	-
−103.4554974	32.00740996	0.57	0.57	0.56	-	0.57	0.61	0.33
−103.4765182	32.01066005	0.28	0.27	0.33	0.15	0.27	0.31	0.21
−103.5147496	32.00953712	0.32	-	0.28	0.67	-	0.42	0.22

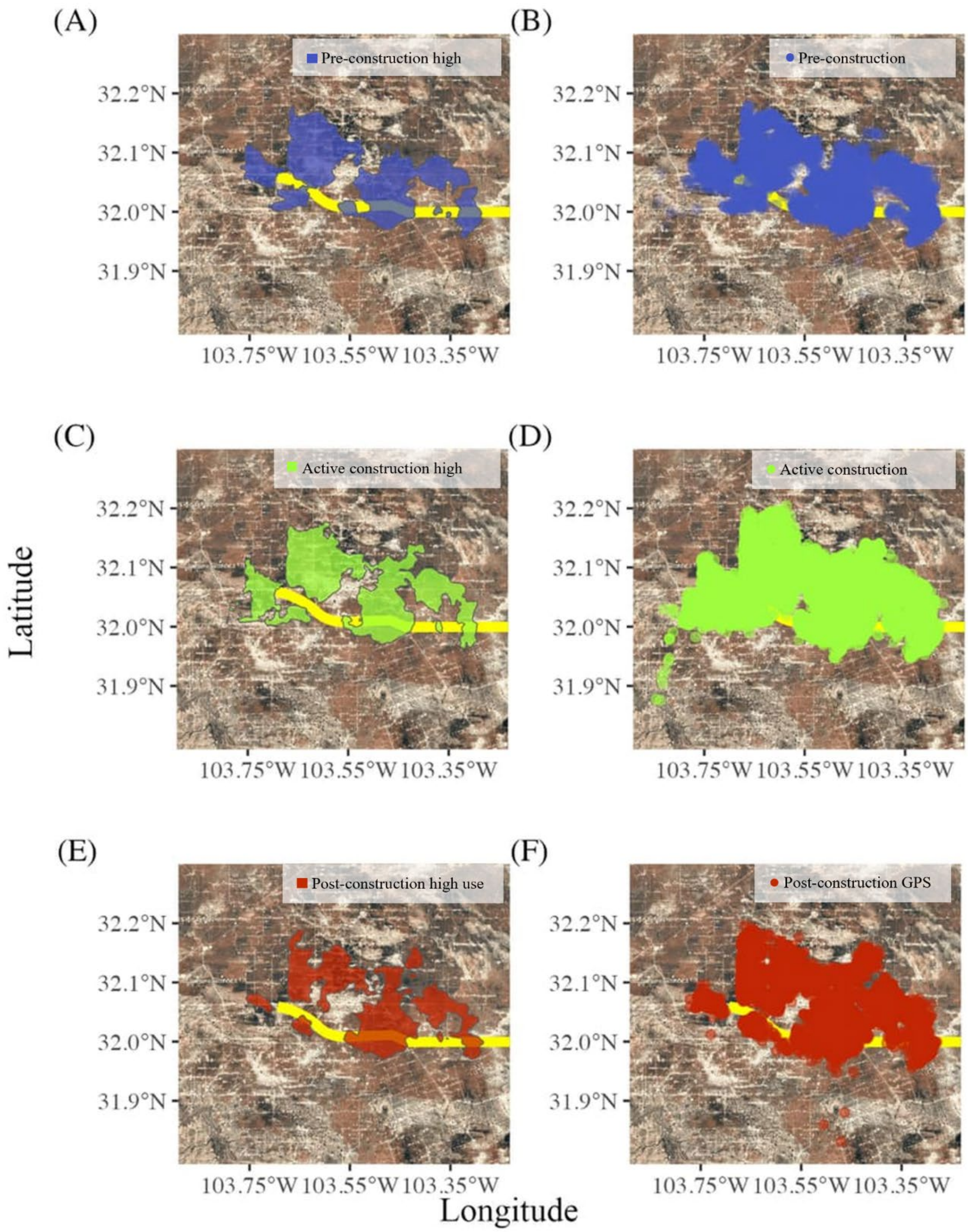

Figure S1. High use area for mule deer derived from averaging individual utilization distributions in the (A) pre-, (C) active, and (E) post-construction phases of the Kermit conveyor belt system in southeast New Mexico, United States. Global positioning system (GPS) locations of adult mule deer collected between 8 March 2022 and 21 February 2025 in the (B) pre- (n = 45,495), (D) active (n = 50,147), and (F) post-phases (n = 13,806) of conveyor belt construction. The location of the conveyor belt (yellow line) is given for reference.

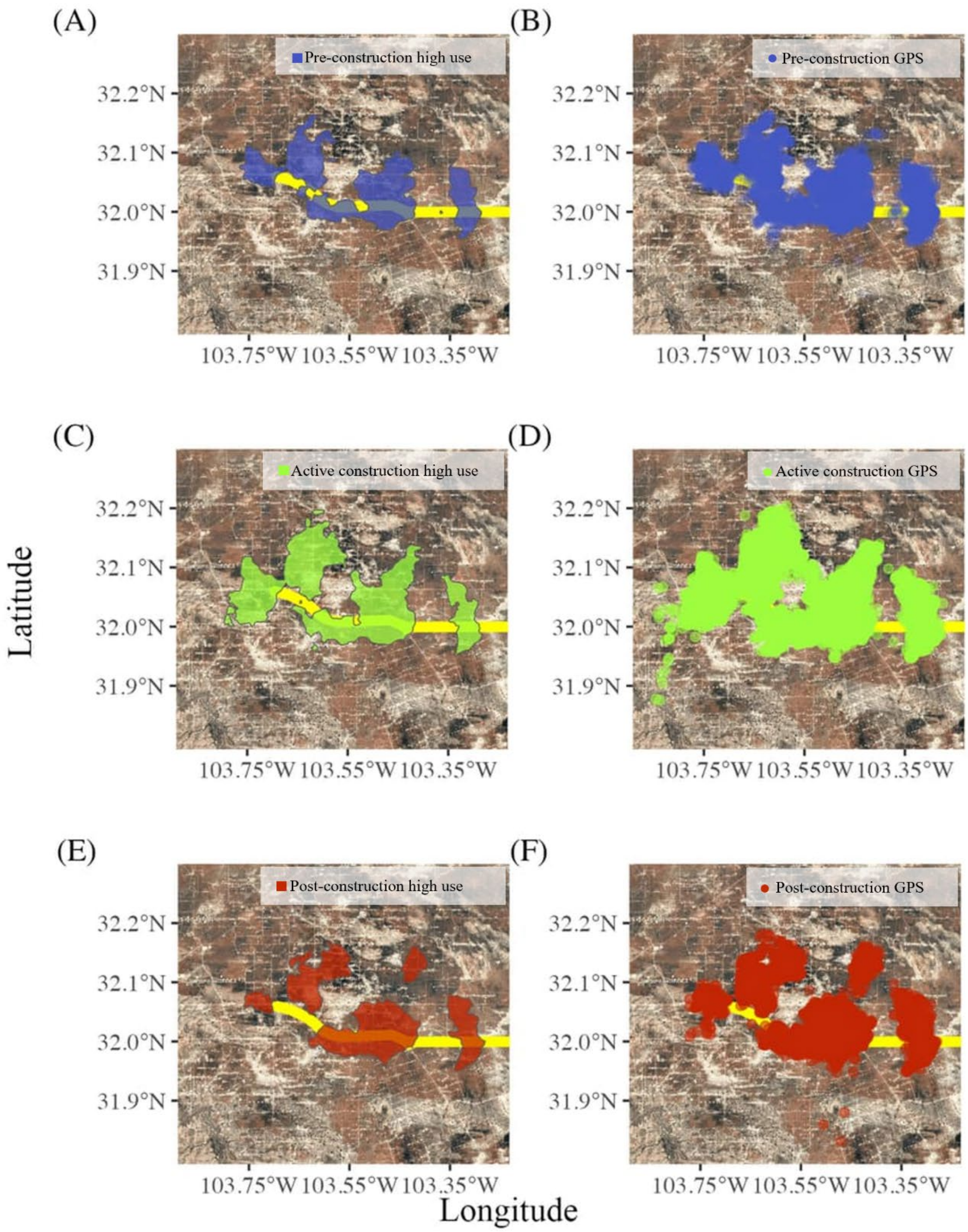

Figure S2. High use area for mule deer derived from averaging individual utilization distributions in the (A) pre-, (C) active, and (E) post-construction phases of the right-of-way for the Kermit conveyor belt system in southeast New Mexico, United States. Global positioning system (GPS) locations of adult mule deer collected between 8 March 2022 and 21 February 2025 in the (B) pre- (n = 30,442), (D) active (n = 35,746) and (F) post-phases (n = 17,680) of the right-of-way construction. The location of the right-of-way for the conveyor belt (yellow solid line) is given for reference.

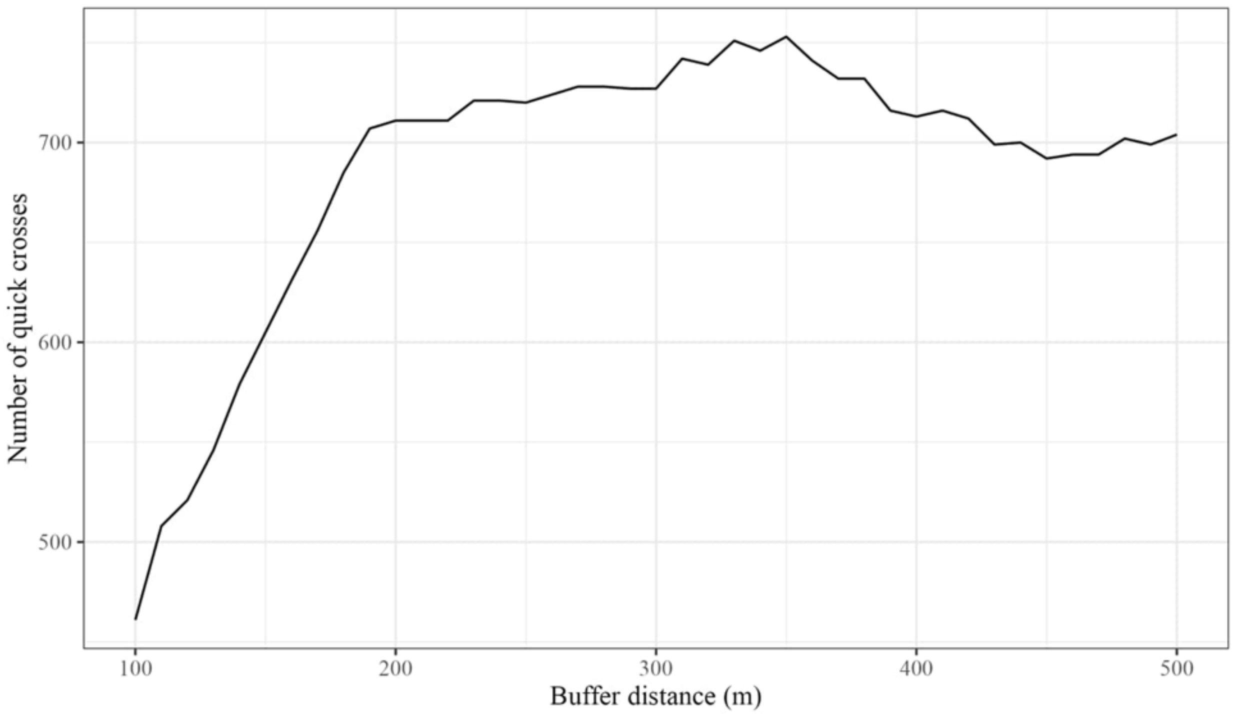

Figure S3. Sensitivity analysis for Barrier Behavior Analysis to determine optimal buffer distance including number of quick crosses vs. buffer distance in meters.

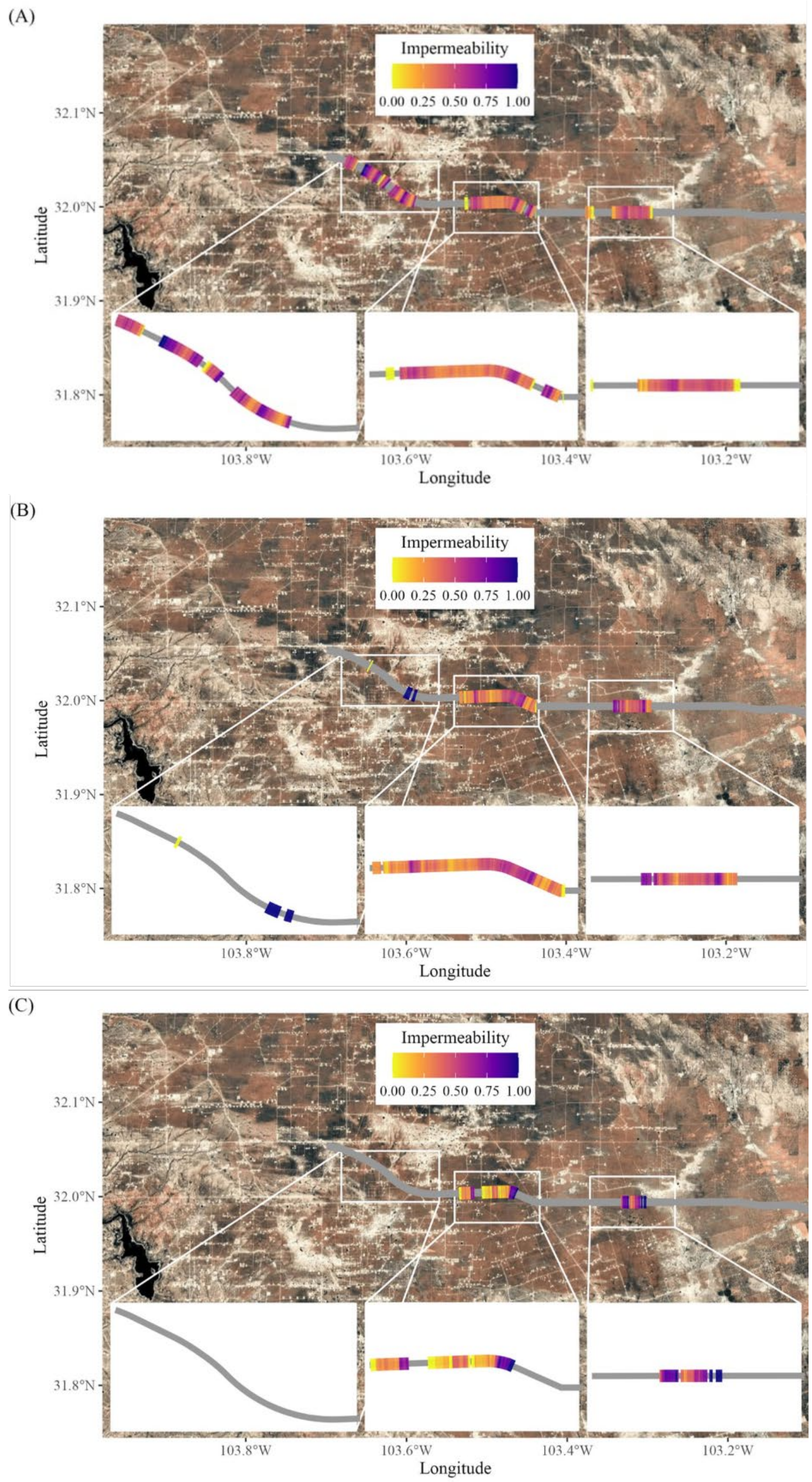

Figure S4. Impermeability index in the (A) pre-, (B) active, and (C) post-phases of conveyor belt construction estimated from barrier behavior analysis for mule deer in southeast New Mexico, United States. The impermeability index was calculated as the ratio of altered movements (bounce, back-and-forth, and trace) to total encounters and rescaled between zero and one.

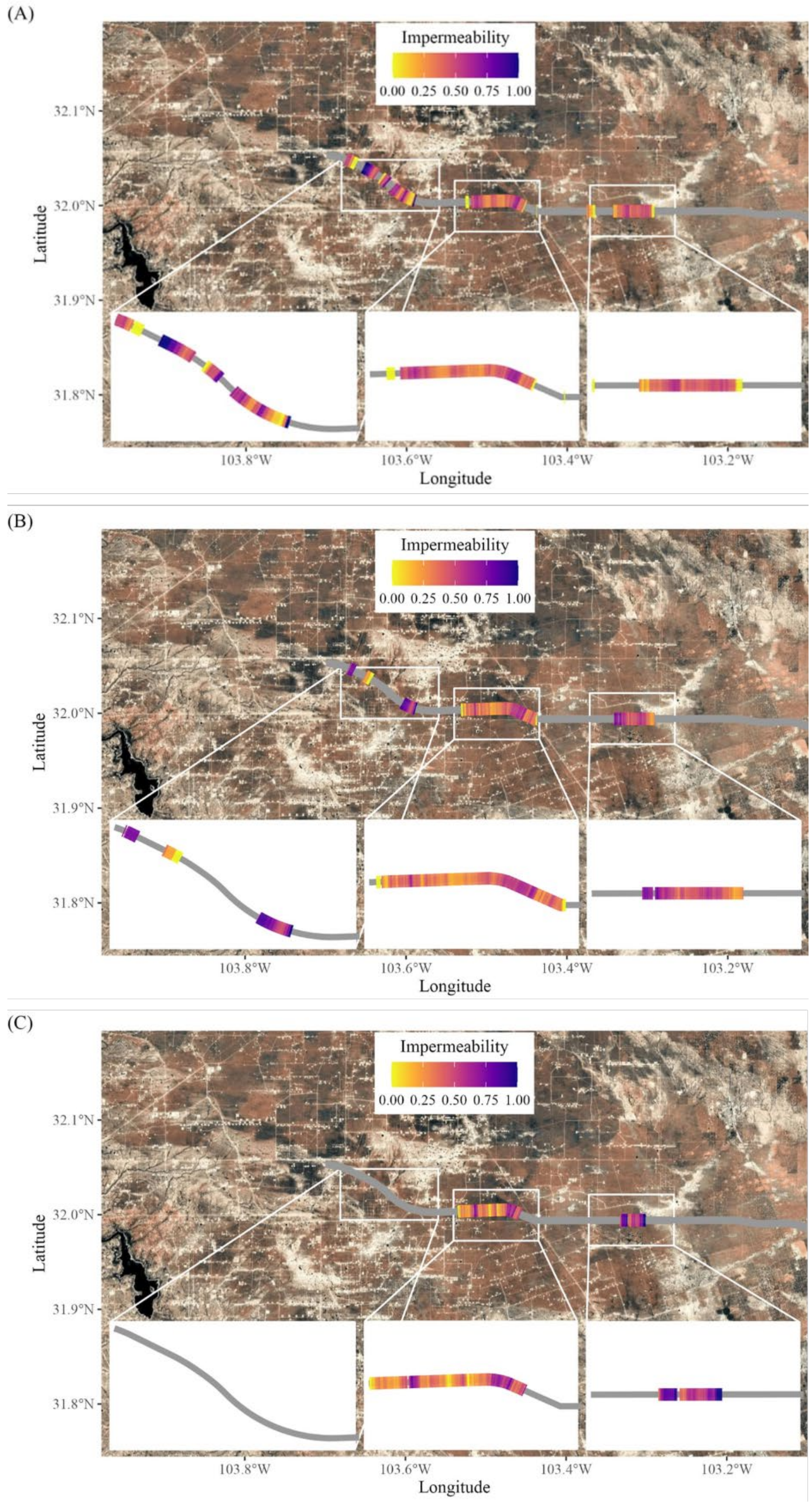

Figure S5. Impermeability index in the (A) pre-, (B) active, and (C) post-phases of right-of-way construction estimated from barrier behavior analysis for mule deer in southeast New Mexico, United States. The impermeability index was calculated as the ratio of altered movements (bounce, back-and-forth, and trace) to total encounters and rescaled between zero and one.